Betz, A., Ashery, U., Rickmann, M., Augustin, I., Neher, E., Sudhof, T.C., Rettig, J., and Brose, N. (1998). Munc13–1 is a presynaptic phorbol ester receptor that enhances neurotransmitter release. Neuron *21*, 123–136.

Betz, A., Thakur, P., Junge, H.J., Ashery, U., Rhee, J.S., Scheuss, V., Rosenmund, C., Rettig, J., and Brose, N. (2001). Functional interaction of the active zone proteins Munc13–1 and RIM1 in synaptic vesicle priming. Neuron *30*, 183–196.

Bito, H., Deisseroth, K., and Tsien, R.W. (1996). CREB phosphorylation and dephosphorylation: a Ca^{2+}- and stimulus duration-dependent switch for hippocampal gene expression. Cell *87*, 1203–1214.

Brown, T.H., Kairiss, E.W., and Keenan, C.L. (1990). Hebbian synapses: biophysical mechanisms and algorithms. Annu. Rev. Neurosci. *13*, 475–511.

Cardozo, T., and Pagano, M. (2004). The SCF ubiquitin ligase: insights into a molecular machine. Nat. Rev. Mol. Cell Biol. *5*, 739–751.

Chin, L.S., Vavalle, J.P., and Li, L. (2002). Staring, a novel E3 ubiquitin-protein ligase that targets syntaxin 1 for degradation. J. Biol. Chem. *277*, 35071–35079.

Coux, O., Tanaka, K., and Goldberg, A.L. (1996). Structure and functions of the 20S and 26S proteasomes. Annu. Rev. Biochem. *65*, 801–847.

DiAntonio, A., Haghighi, A.P., Portman, S.L., Lee, J.D., Amaranto, A.M., and Goodman, C.S. (2001). Ubiquitination-dependent mechanisms regulate synaptic growth and function. Nature *412*, 449–452.

Ehlers, M.D. (2003). Activity level controls postsynaptic composition and signaling via the ubiquitin-proteasome system. Nat. Neurosci. *6*, 231–242.

Hata, Y., and Takai, Y. (1999). Roles of postsynaptic density-95/synapse-associated protein 90 and its interacting proteins in the organization of synapses. Cell. Mol. Life Sci. *56*, 461–472.

Hatanaka, K., Ikegami, K., Takagi, H., and Setou, M. (2006a). Hypoosmotic shock induces nuclear export and proteasome-dependent decrease of UBL5. Biochem. Biophys. Res. Commun. *350*, 610–615.

Hatanaka, T., Hatanaka, Y., and Setou, M. (2006b). Regulation of amino acid transporter ATA2 by ubiquitin ligase NEDD4–2. J. Biol. Chem. *281*, 35922–35930.

Hatanaka, T., Hatanaka, Y., Tsuchida, J.I., Ganapathy, V., and Setou, M. (2006c). Amino acid transporter ATA2 is stored at the trans-Golgi network and released by insulin stimulus in adipocytes. J. Biol. Chem. *281*, 39273–39284.

Hershko, A., and Ciechanover, A. (1998). The ubiquitin system. Annu. Rev. Biochem. *67*, 425–479.

Hsiung, Y.G., Chang, H.C., Pellequer, J.L., La Valle, R., Lanker, S., and Wittenberg, C. (2001). F-box protein Grr1 interacts with phosphorylated targets via the cationic surface of its leucine-rich repeat. Mol. Cell. Biol. *21*, 2506–2520.

Ikegami, K., Mukai, M., Tsuchida, J., Heier, R.L., MacGregor, G.R., and Setou, M. (2006). TTLL7 is a mammalian beta-tubulin polyglutamylase required for growth of MAP2-positive neurites. J. Biol. Chem. *281*, 30707–30716.

Ikegami, K., Heier, R.L., Taruishi, M., Takagi, H., Mukai, M., Shimma, S., Taira, S., Hatanaka, K., Morone, N., Yao, I., et al. (2007). Loss of alpha-tubulin polyglutamylation in ROSA22 mice is associated with abnormal targeting of KIF1A and modulated synaptic function. Proc. Natl. Acad. Sci. USA *104*, 3213–3218.

Ingham, R.J., Gish, G., and Pawson, T. (2004). The Nedd4 family of E3 ubiquitin ligases: functional diversity within a common modular architecture. Oncogene *23*, 1972–1984.

Inoue, E., Mochida, S., Takagi, H., Higa, S., Deguchi-Tawarada, M., Takao-Rikitsu, E., Inoue, M., Yao, I., Takeuchi, K., Kitajima, I., et al. (2006). SAD: A presynaptic kinase associated with synaptic vesicles and the active zone cytomatrix that regulates neurotransmitter release. Neuron *50*, 261–275.

Jin, J., Cardozo, T., Lovering, R.C., Elledge, S.J., Pagano, M., and Harper, J.W. (2004). Systematic analysis and nomenclature of mammalian F-box proteins. Genes Dev. *18*, 2573–2580.

Kaeser, P.S., and Sudhof, T.C. (2005). RIM function in short- and long-term synaptic plasticity. Biochem. Soc. Trans. *33*, 1345–1349.

Kato, A., Fukuda, T., Fukazawa, Y., Isojima, Y., Fujitani, K., Inokuchi, K., and Sugiyama, H. (2001). Phorbol esters promote postsynaptic accumulation of Vesl-1S/Homer-1a protein. Eur. J. Neurosci. *13*, 1292–1302.

Katz, B., and Miledi, R. (1968). The role of calcium in neuromuscular facilitation. J. Physiol. *195*, 481–492.

Kawakami, T., Chiba, T., Suzuki, T., Iwai, K., Yamanaka, K., Minato, N., Suzuki, H., Shimbara, N., Hidaka, Y., Osaka, F., et al. (2001). NEDD8 recruits E2-ubiquitin to SCF E3 ligase. EMBO J. *20*, 4003–4012.

Kosik, K.S. (2006). The neuronal microRNA system. Nat. Rev. Neurosci. *7*, 911–920.

Kreft, M., Kuster, V., Grilc, S., Rupnik, M., Milisav, I., and Zorec, R. (2003). Synaptotagmin I increases the probability of vesicle fusion at low $[Ca^{2+}]$ in pituitary cells. Am. J. Physiol. *284*, C547–C554.

Liao, E.H., Hung, W., Abrams, B., and Zhen, M. (2004). An SCF-like ubiquitin ligase complex that controls presynaptic differentiation. Nature *430*, 345–350.

Matilla, A., Roberson, E.D., Banfi, S., Morales, J., Armstrong, D.L., Burright, E.N., Orr, H.T., Sweatt, J.D., Zoghbi, H.Y., and Matzuk, M.M. (1998). Mice lacking ataxin-1 display learning deficits and decreased hippocampal paired-pulse facilitation. J. Neurosci. *18*, 5508–5516.

Matsumoto, M., Setou, M., and Inokuchi, K. (2007). Transcriptome analysis reveals the population of dendritic RNAs and their redistribution by neural activity. Neurosci. Res. *57*, 411–423.

McCabe, B.D., Hom, S., Aberle, H., Fetter, R.D., Marques, G., Haerry, T.E., Wan, H., O'Connor, M.B., Goodman, C.S., and Haghighi, A.P. (2004). Highwire regulates presynaptic BMP signaling essential for synaptic growth. Neuron *41*, 891–905.

Miyawaki, A., Griesbeck, O., Heim, R., and Tsien, R.Y. (1999). Dynamic and quantitative Ca^{2+} measurements using improved cameleons. Proc. Natl. Acad. Sci. USA *96*, 2135–2140.

Omori, A., Ichinose, S., Kitajima, S., Shimotohno, K.W., Murashima, Y.L., Shimotohno, K., and Seto-Ohshima, A. (2002). Gerbils of a seizure-sensitive strain have a mitochondrial inner membrane protein with different isoelectric points from those of a seizure-resistant strain. Electrophoresis *23*, 4167–4174.

Pak, D.T., and Sheng, M. (2003). Targeted protein degradation and synapse remodeling by an inducible protein kinase. Science *302*, 1368–1373.

Pickart, C.M. (2001). Mechanisms underlying ubiquitination. Annu. Rev. Biochem. *70*, 503–533.

Schoch, S., Castillo, P.E., Jo, T., Mukherjee, K., Geppert, M., Wang, Y., Schmitz, F., Malenka, R.C., and Sudhof, T.C. (2002). RIM1alpha forms a protein scaffold for regulating neurotransmitter release at the active zone. Nature *415*, 321–326.

Setou, M., Nakagawa, T., Seog, D.H., and Hirokawa, N. (2000). Kinesin superfamily motor protein KIF17 and mLin-10 in NMDA receptor-containing vesicle transport. Science *288*, 1796–1802.

Setou, M., Seog, D.H., Tanaka, Y., Kanai, Y., Takei, Y., Kawagishi, M., and Hirokawa, N. (2002). Glutamate-receptor-interacting protein GRIP1 directly steers kinesin to dendrites. Nature *417*, 83–87.

Sudhof, T.C. (2004). The synaptic vesicle cycle. Annu. Rev. Neurosci. *27*, 509–547.

Varshavsky, A. (2005). Regulated protein degradation. Trends Biochem. Sci. *30*, 283–286.

Wang, Y., Okamoto, M., Schmitz, F., Hofmann, K., and Sudhof, T.C. (1997). Rim is a putative Rab3 effector in regulating synaptic-vesicle fusion. Nature *388*, 593–598.

Wheeler, T.C., Chin, L.S., Li, Y., Roudabush, F.L., and Li, L. (2002). Regulation of synaptophysin degradation by mammalian homologues of seven in absentia. J. Biol. Chem. *277*, 10273–10282.

Willeumier, K., Pulst, S.M., and Schweizer, F.E. (2006). Proteasome inhibition triggers activity-dependent increase in the size of the recycling vesicle pool in cultured hippocampal neurons. J. Neurosci. *26*, 11333–11341.

Winston, J.T., Koepp, D.M., Zhu, C., Elledge, S.J., and Harper, J.W. (1999). A family of mammalian F-box proteins. Curr. Biol. *9*, 1180–1182.

Yao, I., Hata, Y., Hirao, K., Deguchi, M., Ide, N., Takeuchi, M., and Takai, Y. (1999). Synamon, a novel neuronal protein interacting with synapse-associated protein 90/postsynaptic density-95-associated protein. J. Biol. Chem. *274*, 27463–27466.

Yao, I., Iida, J., Nishimura, W., and Hata, Y. (2002). Synaptic and nuclear localization of brain-enriched guanylate kinase-associated protein. J. Neurosci. *22*, 5354–5364.

Yi, J.J., and Ehlers, M.D. (2005). Ubiquitin and protein turnover in synapse function. Neuron *47*, 629–632.

Zhang, F.L., and Casey, P.J. (1996). Protein prenylation: molecular mechanisms and functional consequences. Annu. Rev. Biochem. *65*, 241–269.

MOLECULAR AND CELLULAR BIOLOGY, Jan. 2008, p. 293–301 Vol. 28, No. 1
0270-7306/08/$08.00+0 doi:10.1128/MCB.00473-07

Altered Quality Control in the Endoplasmic Reticulum Causes Cortical Dysplasia in Knock-In Mice Expressing a Mutant BiP▽

Naoya Mimura,[1,2] Shigeki Yuasa,[3] Miho Soma,[3] Hisayo Jin,[1] Keita Kimura,[2] Shigemasa Goto,[2] Haruhiko Koseki,[4] and Tomohiko Aoe[1]*

Department of Anesthesiology[1] and Department of Medicine and Clinical Oncology,[2] Chiba University Graduate School of Medicine, 1-8-1 Inohana, Chuo-ku, Chiba City, Chiba 260-8670, Department of Ultrastructural Research, National Institute of Neuroscience, National Center of Neurology and Psychiatry, 4-1-1 Ogawahigashi, Kodaira, Tokyo 187-8502,[3] and Laboratory for Developmental Genetics, RIKEN Research Center for Allergy and Immunology, 1-7-22 Suehiro, Tsurumi, Yokohama 230-0045,[4] Japan

Received 20 March 2007/Returned for modification 21 June 2007/Accepted 2 October 2007

Binding immunoglobulin protein (BiP) is an endoplasmic reticulum (ER) molecular chaperone that is central to ER function. We examined knock-in mice expressing a mutant BiP in order to elucidate physiological processes that are sensitive to BiP functions during development and adulthood. The mutant BiP lacked the retrieval sequence that normally functions to return BiP to the ER from the secretory pathway. This allowed us to examine the effects of a defect in ER function without completely eliminating BiP function. The homozygous mutant BiP neonates died after birth due to respiratory failure. Besides that, the mutant BiP mice displayed disordered layer formation in the cerebral cortex and cerebellum, a neurological phenotype of *reeler* mutant-like malformation. Consistent with the phenotype, Cajal-Retzius (CR) cells did not secrete reelin, and the expression of reelin was markedly reduced posttranscriptionally. Furthermore, the reduction in the size of the whole brain and the apparent scattering of CR cells throughout the cortex, which were distinct from the *reeler* phenotype, were also seen. These findings suggest that the maturation and secretion of reelin in CR cells and other factors related to neural migration may be sensitive to aberrant ER quality control, which may cause various neurological disorders.

Proteins destined for the secretory pathway are inserted into the endoplasmic reticulum (ER) cotranslationally and subjected to quality control (12, 25). Aberrant protein folding due to extracellular stimuli such as ischemia, hypoxia, and genetic mutations results in the accumulation of misfolded proteins in the ER, which causes ER stress and initiates the unfolded protein response (UPR) (35, 39) that enhances the capacity for ER quality control by reducing general protein synthesis (18), producing ER chaperones, and promoting ER-associated degradation (4, 6). A failure of this adaptation mechanism may cause cellular dysfunction and cell death, resulting in diverse human disorders (24, 26) such as neurodegenerative disease (21, 23), cardiomyopathy (15), and diabetes (17, 34). Furthermore, mutant mouse models have revealed that the UPR plays a vital role during normal development by increasing protein synthesis, as necessary, of dedicated secretory cells (46) such as pancreatic beta cells (38), plasma cells (37), hepatocytes (36), and alveolar type II epithelial cells (29). Inadequate adaptation to these physiological demands may lead to diverse diseases.

ER molecular chaperones and folding enzymes such as binding immunoglobulin protein (BiP), calnexin, and protein disulfide isomerase facilitate the correct folding or degradation of these newly synthesized proteins as well as of misfolded proteins. BiP, also called the 78-kDa glucose-regulated protein (GRP78), is a member of the heat shock protein 70 (HSP70) family of proteins and is one of the most abundant ER chaperones, assisting in protein translocation, folding, and degradation (31). ER chaperones localize to the ER by two mechanisms: retention and retrieval (40). BiP is retained in the ER by interacting with other ER proteins and the ER matrix. When misfolded proteins accumulate in the ER, BiP is secreted from the ER together with the misfolded proteins, where it assists with protein refolding, or it helps in the degradation of these proteins (16, 47). In post-ER compartments, the carboxyl-terminal Lys-Asp-Glu-Leu (KDEL) sequence of BiP is then recognized by the KDEL receptor, which facilitates the return of BiP to the ER (27, 30).

The complete depletion of BiP has lethal effects on mammalian early embryonic cells (28). *Saccharomyces cerevisiae* BiP (Kar2p) is essential for survival, while the deletion of the retrieval sequence (His-Asp-Glu-Leu [HDEL] in yeast) is dispensable because the UPR is activated, and the loss of the chaperone in the ER is compensated for (3). Therefore, to elucidate physiological processes that are sensitive to BiP functions during development and adulthood in multicellular organisms, we produced knock-in mice expressing a mutant BiP in which the retrieval sequence was deleted by homologous recombination. The mutant BiP mice died within several hours after birth due to impaired pulmonary surfactant biosynthesis and respiratory failure (29). We also found disordered layer formation in the cerebral cortex and cerebellum in the mutant BiP neonates. Although altered quality control in the ER due to mutant BiP may affect the expression of several proteins with regard to corticogenesis, we found that the expression of one such protein, reelin, secreted by Cajal-Retzius (CR) cells (9), was markedly reduced. These findings suggest that committed secretory cells, such as CR cells, have a threshold of

* Corresponding author. Mailing address: Department of Anesthesiology, Chiba University Graduate School of Medicine, 1-8-1 Inohana, Chuo-ku, Chiba City, Chiba 260-8670, Japan. Phone: 81-43-226-2573. Fax: 81-43-226-2156. E-mail: taoe@faculty.chiba-u.jp.

▽ Published ahead of print on 22 October 2007.

protein-folding capacity to cope with the normal physiological protein overload in the ER during development, and BiP plays an important role.

MATERIALS AND METHODS

Reagents. The following antibodies were used: mouse monoclonal antibody (mAb) CR50 against reelin (a gift from M. Ogawa, Brain Science Institute, RIKEN, Japan), rabbit antiserum against the hemagglutinin (HA) epitope (Zymed, San Francisco, CA), mouse mAb G10 against reelin, rabbit antiserum against Dab1 (Chemicon, Temecula, CA), rabbit antiserum against Dab1 (phospho-Y220) (Abcam, Cambridge, United Kingdom), mouse mAb EP5 against fibronectin, mouse mAb 6A6 against very-low-density lipoprotein receptor (VLDLR), rabbit antiserum against CHOP/GADD153, rabbit antiserum against ubiquitin, goat polyclonal antiserum against BiP/GRP78, mouse mAb J-3 against Cdk5 (Santa Cruz Biotechnology, Santa Cruz, CA), mouse mAb 9E10 against the Myc epitope (ATCC, Manassas, VA), mouse mAb against γ-tubulin (Sigma Chemical, St. Louis, MO), mouse mAb SPA-827 against BiP (KDEL sequence) (Stressgen, Ann Arbor, MI), Cy2-conjugated donkey antibody against rabbit immunoglobulin G (IgG), and Cy3-conjugated donkey antibody against mouse IgG (Jackson Immunoresearch Laboratories, West Grove, PA). TO-PRO-3 and a Slow-Fade antifade kit were purchased from Molecular Probes (Invitrogen, Carlsbad, CA).

Plasmids and transfection. A *reelin* cDNA (pCrl) was kindly provided by T. Curran (St. Jude Children's Research Hospital, Memphis, TN) (10). To express a Myc-tagged mutant BiP lacking the KDEL sequence, a cDNA encoding a mutant BiP with residues 1 to 650 was obtained by PCR using rat *BiP* cDNA (a gift from H. R. B. Pelham, MRC Laboratory of Molecular Biology, United Kingdom). The PCR product was subcloned into a pcDNA3.1 Myc-His vector (Invitrogen, Carlsbad, CA). Transfection was performed with the calcium phosphate method (20).

Mutant BiP mice. We used homologous recombination to establish knock-in mice expressing BiP lacking the carboxyl-terminal KDEL sequence (29). The missing KDEL sequence was replaced by an HA tag. All animal experimental procedures were performed in accordance with a protocol approved by the Institutional Animal Care Committee of Chiba University, Chiba, Japan.

Western blot. The brains removed from the mice and cells were homogenized in a buffer containing 0.4% Nonidet P-40, 0.2% *N*-lauroylsarcosine, 30 mM Tris-HCl (pH 8.0), 1 mM EDTA, 10 μg ml^{-1} aprotinin, 10 μg ml^{-1} leupeptin, and 30 μg ml^{-1} *N*-acetyl-L-leucinal-L-lecinal-L-norleucinal (ALLN; Sigma Chemical). The lysates were boiled in sodium dodecyl sulfate-polyacrylamide gel electrophoresis sample buffer and separated by sodium dodecyl sulfate-polyacrylamide gel electrophoresis under reducing conditions. Gels were transferred onto polyvinylidene fluoride membranes (Immobilon-P; Millipore Corp., Billerica, MA), blocked with 5% nonfat dry milk in the buffer described above, incubated with a primary antibody followed by peroxidase-conjugated donkey anti-goat, anti-mouse, or anti-rabbit IgG, and developed by chemiluminescence (ECL; Amersham Pharmacia Biotech, Buckinghamshire, United Kingdom). Imaging was obtained by using LAS1000 and Image Gauge software (Fuji Photo Film Co. Ltd., Tokyo, Japan).

Primary neuronal culture. Cortical neurons of mouse embryos were derived from embryos at day 17.5 to 18.5 according to standard procedures (1). After removing the meninges, cortical lobes were isolated in phosphate-buffered saline (PBS), dissected into small pieces, and digested with 0.25% trypsin and 0.02% DNase I in PBS with 5% glucose at 37°C for 20 min. Trypsin was then neutralized with a half volume of horse serum, and the solution was centrifuged at 440 × *g* for 5 min at 4°C. The resultant cells were triturated in Dulbecco's modified Eagle's medium (DMEM)–F-12 medium containing 10% fetal bovine serum using a siliconized Pasteur pipette and scattered at about 2×10^5 to 4×10^5 cells/cm^2 on plates coated with poly-L-lysine (Sigma). Cells were maintained in DMEM–F-12 medium containing 10% fetal bovine serum–1% penicillin-streptomycin for 3 days at 37°C and then replaced with opti-MEM (Invitrogen) containing 1% of an insulin-transferrin-selenium A mixture (ITS; Invitrogen) and antibiotics. On the following day, the supernatants were collected, centrifuged using a table-top machine at 440 × *g* for 5 min at 4°C, and concentrated by centrifugation (YM50; Millipore). The neurons were treated with control or reelin-containing medium (prepared as previously described) (8) at 37°C for 20 min and collected for Western blotting. 293T cells were transfected with full-length mouse reelin expression construct pCrl. The following day, the cells were washed with serum-free DMEM and maintained in opti-MEM containing 1% ITS and antibiotics. After three more days, the conditioned medium was collected, centrifuged at 440 × *g* for 5 min at 4°C, and used as the reelin-containing medium.

Confocal and immunofluorescence microscopy of primary neurons. Cells on coverslips were fixed in cold methanol for 10 min at −20°C and then processed as previously described (20). The stained cells were examined by either confocal laser scanning microscopy (LSM510 fitted with krypton and argon lasers; Carl Zeiss, Oberkochen, Germany) or fluorescence microscopy (Axiovert 200 M; Carl Zeiss).

Northern blot. Northern blot analysis was done as previously described (15). The expression level of the *reelin* and *BiP* mRNAs was assessed relative to that of β-*actin* mRNA using densitometry by Image Gauge software (Fuji Photo Film).

In situ hybridization histochemistry. *reelin* cDNA extending from nucleotides 4716 to 5476 (GenBank accession number U24703) (9) was cloned into the pGEM-T Easy vector (Promega, Madison, WI). In vitro transcription from *reelin* cDNA was performed using a digoxigenin-UTP RNA labeling kit (Roche Applied Science, Mannheim, Germany) to prepare the antisense and sense cRNA probes according to the manufacturer's instructions.

The brains of mouse embryos at embryonic day 15.5 (E15.5) were fixed with 4% paraformaldehyde dissolved in 0.1 M sodium phosphate buffer (pH 7.4), and postfixed overnight at 4°C with the same fixative. The brains were embedded in 2% agar in PBS and sliced coronally into 150-μm sections with a Microslicer (DTK-3000; Dosaka EM, Kyoto, Japan). Hybridization and detection procedures were performed as described below. The free-floating sections were incubated with proteinase K (20 μg/ml) in 0.1% Tween 20 in PBS (PBST) for 10 min at room temperature. Sections were rinsed with PBST, refixed in 4% paraformaldehyde for 20 min, and again rinsed with PBST three times each for 20 min. Sections were prehybridized in hybridization buffer (50% formamide, 5× SSC [1× SSC is 0.15 M NaCl plus 0.015 M sodium citrate], 50 μg/ml heparin, 0.1% Tween 20, 5 mg/ml torula RNA) for 30 min at 65°C. Subsequently, sections were hybridized overnight at 65°C with digoxigenin-UTP-labeled antisense or sense riboprobes (0.2 μg/ml) in the hybridization buffer. Sections were then sequentially rinsed in 2× SSCT (0.1% Tween 20 in SSC)–50% formamide twice each for 30 min at 65°C, 2× SSCT for 15 min at 65°C, and 0.2× SSCT twice each for 30 min at 65°C and then incubated overnight with alkaline phosphatase-coupled anti-digoxigenin antibody (1:4,000 dilution; Roche Applied Science, Mannheim, Germany). After washing with PBST three times and then once with 0.1 M Tris-HCl (pH 8.2), sections were stained by use of a solution prepared from FastRed tablets (Roche Applied Science, Mannheim, Germany) according to the manufacturer's instruction and then washed with PBST three times. Sections were then coverslipped with 80% glycerol, and fluorescence images were obtained directly with a confocal laser scanning microscope (LSM5 Pa; Zeiss, Oberkochen, Germany). No labeling was detectable in the control sections that were hybridized with the sense riboprobe (data not shown).

Immunohistochemistry. Pregnant mice were deeply anesthetized by Nembutal, and embryos were removed by cesarean section. The embryos were fixed by transcardiac perfusion with 4% paraformaldehyde in PBS, and the heads were further immersion fixed for 12 h at 4°C. Embryonic brains were then embedded in 3% agar in PBS, and sections at a thickness of 200 μm were prepared on a Microslicer (Dosaka EM, Kyoto, Japan). The sections were incubated with 10% normal goat serum in PBS for 30 min to block nonspecific antibody binding and then incubated with a mixture of CR50 mouse monoclonal antibody (1:200 dilution) (32) and rabbit anti-calretinin (1:2,000; Swant, Switzerland) in PBS for 12 h at 4°C. The sections were rinsed with PBS and then incubated with a mixture of Cy2-conjugated anti-rabbit IgG (1:100; Jackson Immunoresearch) and Cy3-conjugated anti-mouse IgG (1:200; Chemicon) in PBS for 2 h at 4°C. For calbindin immunohistochemistry of the cerebellum, rabbit anti-calbindin (1:2,000; Swant) was used as the primary antibody, and Cy2-conjugated anti-rabbit IgG was the secondary antibody. The sections were then rinsed with PBS and mounted onto glass slides with 80% glycerol. For counterstaining with a DNA dye, the sections immunostained with anti-calbindin antibody were stained with TO-PRO-3 (Invitrogen) and mounted with SlowFade (Molecular Probes). The sections were observed under a confocal laser scanning microscope (LSM5 Pa; Carl Zeiss).

BrdU labeling. Bromodeoxyuridine (BrdU) (80 mg · kg^{-1}) was administered intraperitoneally to pregnant mice at the E13 or E15 three times a day (at 10:00, 16:00, and 22:00). At E18, the embryos were removed by cesarean section and perfusion fixed as mentioned above. The brains were embedded in agar, and sections with a thickness of 200 μm were prepared and incubated with 2 N HCl for 1 h at room temperature. The sections were then rinsed with PBS, treated with 10% normal goat serum, and then incubated with a mouse mAb against BrdU (1:50; Becton Dickinson, San Jose, CA) for 12 h. After rinsing with PBS, the sections were incubated with Alexa 488-conjugated goat anti-mouse IgG

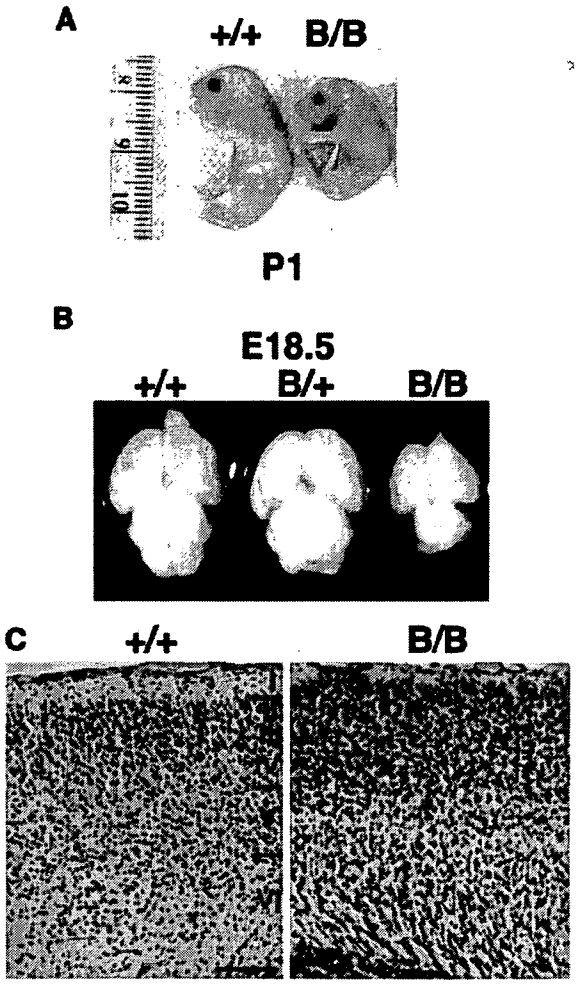

FIG. 1. Absence of the KDEL retrieval sequence from BiP impairs brain development. (A) Newborns at P1. (B) Brains from E18.5 embryos. (C) At E18, large numbers of neurons are distributed in the superficial layer of the mutant (right), in contrast to the cell-sparse layer I of the control (left). (C) Hematoxylin-eosin staining. Scale bar, 100 μm. B/B, homozygous; B/+, heterozygous; +/+, wild type.

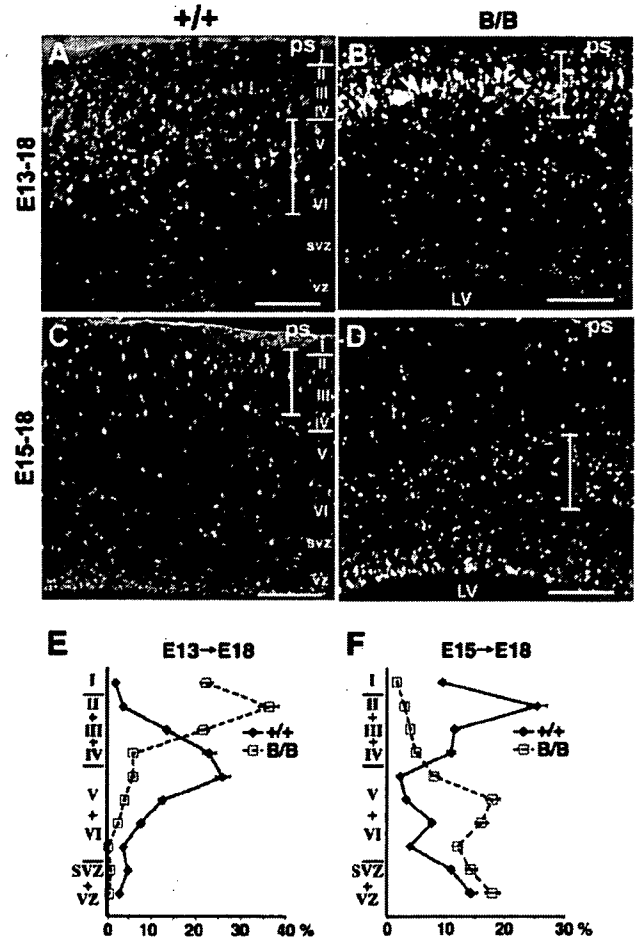

FIG. 2. Mutant BiP mice exhibit an outside-in pattern of neocortical layer formation. Shown is birth date analysis of the neocortical neurons. (A, B, and E) BrdU was administered at E13, and the distribution of the labeled cells was examined at E18. In control mice, heavily labeled cells were stratified in the lower layers (layers V and VI) (A), in contrast to the significant reduction of labeled cells in the lower layers and their significant increase in the superficial layer in the mutant (B). A quantitative analysis is represented in E. (C, D, and F) BrdU was administered at E15, and the distribution of the labeled cells was examined at E18. In the control, heavily labeled cells reached the upper layers (layers II and III), and the still-migrating cells were also found in the lower layer (C). In contrast, only small numbers of the labeled cells reached the upper layers (layers II and III), and a large proportion of them were distributed in the lower layer in the mutant (D). A quantitative analysis is represented in F. The graphs in E and F represent the averages ± standard errors of the means of BrdU-labeled cells in each layer of four serial sections from a representative brain of each genotype. The extent of the layers in that the cortical neurons were intensely labeled with BrdU is indicated by a vertical bar in each picture. B/B, homozygous mutant; +/+, wild-type mice; LV, lateral ventricle; ps, pial surface; svz, subventricular zone; vz, ventricular zone; I to VI, neocortical layers. Scale bars, 100 μm.

(1:500 dilution; Invitrogen) in PBS for 2 h at 4°C. The sections were then rinsed again with PBS and mounted onto glass slides with glycerol. Immunolocalization was observed under a confocal laser scanning microscope. The primordium of the somatosensory cortex was divided into 10 layers from the ventricular surface to the pial surface. The densities of BrdU-labeled cells in each layer were determined in four serial sections from a representative brain of each genotype. BrdU-labeled cells in the defined area of each section of the neocortical primordium were counted from the ventricular surface to the pial surface to obtain the total numbers of labeled cells, and the average percentages of the labeled cells in each layer were plotted on a histogram.

RESULTS

Defective neocortical layer formation in mutant BiP mice. The homozygous mutant BiP mice were born at the expected Mendelian ratio, and they died within 1 day after birth due to respiratory failure (29). They moved and responded to painful stimuli but appeared pale and were significantly smaller than wild-type mice (Fig. 1A). Among the various organs, the mutant brain, including the cerebral cortex and cerebellum, was substantially smaller than those of wild-type mice (Fig. 1B), suggesting that the brain was particularly affected by the BiP mutation. In fact, the neocortical stratification at E18, as observed with hematoxylin-eosin staining, was defective in the mutant BiP mice. The mutant brain had a relatively high density of neurons in neocortical layer I (Fig. 1C, right), in contrast

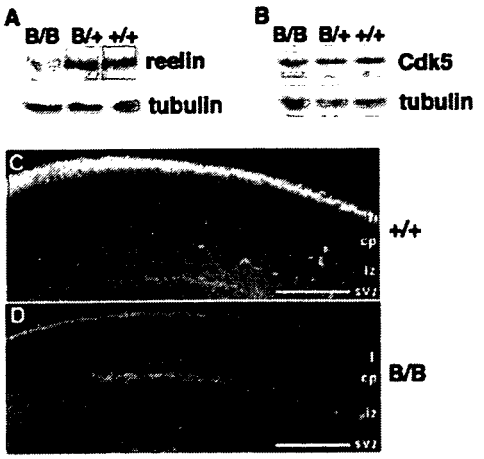

FIG. 3. Significant downregulation of reelin expression in superficial layer I of the mutant BiP neocortical primordium. (A and B) The levels of expression of reelin, Cdk5, and γ-tubulin in brains of E18.5 embryos were evaluated by Western blotting. (C and D) At E16, intense reelin immunoreactivity was found in the superficial layer of the control (C), but immunoreactivity was significantly reduced in the mutant brain (D). Scale bars, 200 μm. cp, cortical plate; iz, intermediate zone; svz, subventricular zone; I, layer I; B/B, homozygous mice; B/+, heterozygous mutant mice; +/+, wild-type mice.

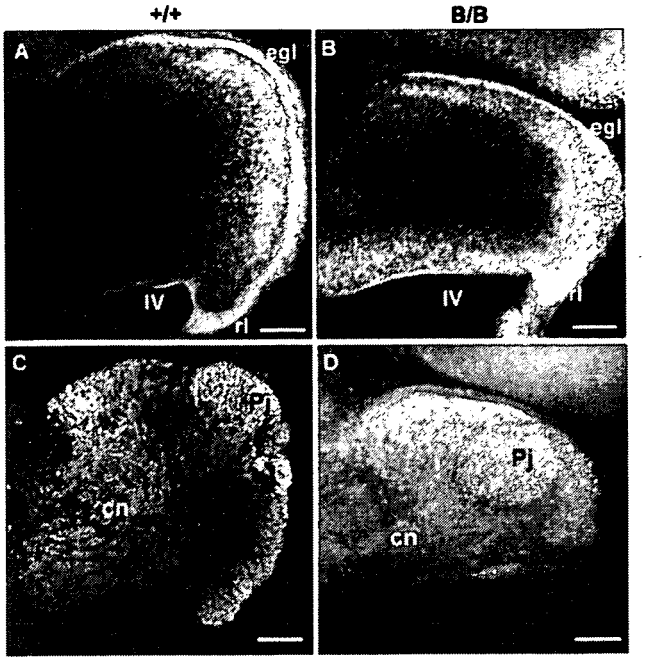

FIG. 4. Mutant BiP mice exhibit defective cerebellar development. (A and B) Staining of the cerebellar primordium at E18 with a DNA dye, TO-PRO-3. The cerebellum of the homozygote (B) is much smaller than that of the wild type (A). An EGL is formed in both genotypes, but the progression of EGL formation in the caudorostral direction is retarded in the homozygote (B). (C and D) Purkinje cell distribution in the cerebellum at E18. Calbindin-immunoreactive Purkinje cells are distributed in the cortical layer in the cerebellum of the control (C). In contrast, large numbers of immunoreactive cells stay in the subcortical region of the mutant cerebellum (D). Scale bars, 100 μm. B/B, homozygous mice; +/+, wild-type mice; cn, cerebellar nucleus; egl, EGL; Pj, Purkinje cell layer; rl, rhombic lip; IV, the fourth ventricle.

to a low density of neuronal arrangement in the control (Fig. 1C, left).

Cortical neurogenesis occurs in the ventricular zone, and the new neurons migrate through other new neurons to the marginal zone and then move to their final destination during embryogenesis. To further investigate the defect in layer formation during neocortical development, birth date analysis of the neocortical neurons was carried out by BrdU labeling (Fig. 2A to D). Neuronal precursors in the ventricular zone became labeled with BrdU during proliferation and migrated after the final mitosis through earlier-born neurons to the cortical plate in normal corticogenesis. When BrdU was administered at E13, heavily labeled cells were distributed in forming layers V and VI, and lightly labeled cells that repeated mitosis after BrdU incorporation were distributed in the upper layers at E18 in the control (Fig. 2A and E), as reported previously by Caviness (7). In the mutant, however, heavily labeled cells were distributed in the upper layer up to superficial layer I, and few labeled cells were observed in the lower layer at E18 (Fig. 2B and E). When BrdU was administered at E15, in the control, the heavily labeled cells reached upper layers II and III at E18 (Fig. 2C and F), as reported previously by Caviness (7), but in the mutant, only a small number of heavily labeled cells reached these upper layers, and most of the labeled cells were distributed in the lower layer (Fig. 2D and F). These findings indicate that, in the mutant brain, the earlier-born neurons reached the superficial layer and remained there and that the later-born neurons did not reach the upper layer, remaining in the lower layer. The mutant BiP mice exhibited an outside-in pattern of neocortical layer formation, in contrast to the inside-out pattern in the control (7), indicating that neocortical layer formation was impaired.

Mutant BiP mice have reduced expression of reelin. The above-described findings suggested that aberrant neocortical formation is due to the defects in layer formation, like a deficiency in reelin signaling in a *reeler* mutant malformation (9, 13) or a deficiency in Cdk5 signaling (33). Indeed, analysis of the embryonic cerebral neocortex revealed significantly reduced reelin expression by Western blotting and immunoreactivity in superficial layer I of the mutant BiP mice (Fig. 3A, C, and D), while the expression of Cdk5 was preserved (Fig. 3B). These results are consistent with the fact that reelin is a secretory protein that may interact with BiP in the ER, whereas Cdk5 is a cytosolic protein that is apart from BiP.

Because *reeler* malformation is also well documented in the cerebellum with regard to the migration defect of Purkinje cells (48), the structure of the cerebellum was examined at E18. The growth of the mutant cerebellum was significantly retarded as shown by staining with DNA dye (Fig. 4A and B). Although the external granular layer (EGL) was formed in both genotypes, the development of an EGL migrating tangentially from the rhombic lip was significantly retarded in the mutant BiP mice (Fig. 4A and B). A large number of Purkinje cells remained in the subcortical region, in contrast to the cortical arrangement of Purkinje cells in the control (Fig. 4C and D). Hippocampal layer formation showed little defect in the mutant BiP mice based on hematoxylin-eosin-stained sections (data not shown).

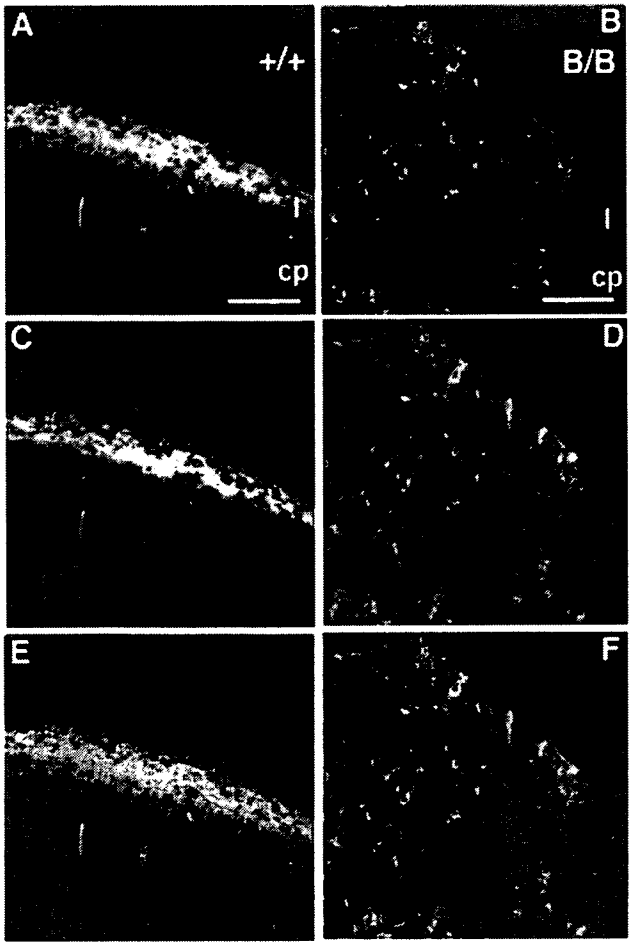

FIG. 5. Distribution of CR cells in the neocortical primordium. At E16, reelin immunoreactivity (red) in the superficial layer (I) of control (A) and mutant (B) brains was present. Calretinin-immunopositive CR cells (green) were found in the superficial layers of both control (C) and mutant (D) mice. Reelin immunoreactivity colocalizes with calretinin in CR cells in the control (E) (A and C were merged), but reelin immunoreactivity is hardly detectable in the calretinin-positive cells in superficial layer I of the mutant (F) (B and D were merged). Furthermore, the cells that were double labeled with reelin and calretinin were found in the layers below the superficial layer in the mutant (F), although such cells were not detected in the wild type (E). Scale bars, 50 μm.

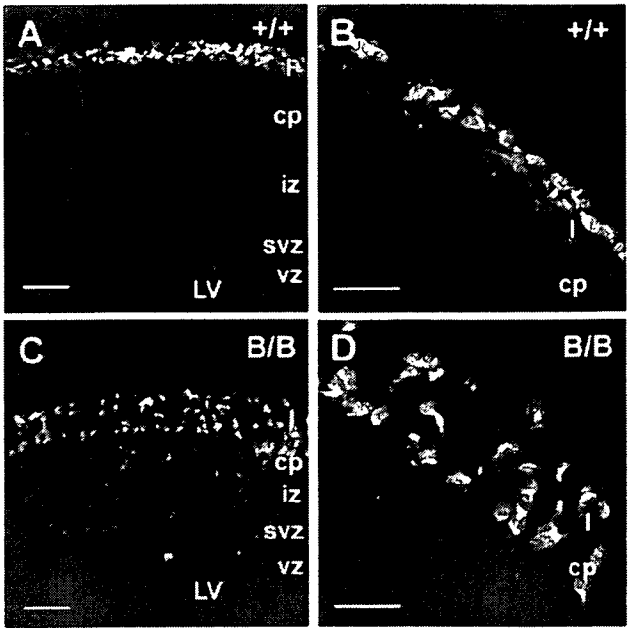

FIG. 6. The cells positive for *reelin* mRNA were scattered in the neocortical primordium of mutant BiP mice. The distribution of CR cells was further confirmed by in situ hybridization for *reelin* mRNA as the marker of CR cells in the neocortical primordium at E15.5. In the control, *reelin* mRNA-positive cells were situated in the superficial layer (layer I) as shown in A. The higher magnification of the upper cortical area represents the characteristic horizontal arrangement of CR cells (B). In contrast, *reelin* mRNA-positive cells were distributed from the superficial layer into the cortical plate in the homozygote (C). (D) Higher magnification of the upper cortical area in C. The random orientation of *reelin*-positive cells is evident. Scale bars, 100 μm in A and C and 50 μm in B and D.

The structure of the superficial layer of the neocortical primordium was further examined by double immunohistochemical labeling for both reelin and calretinin. Calretinin-immunopositive neurons, corresponding to CR cells in the neocortical primordium, were found in the superficial layer of the mutant BiP mice, but their numbers were significantly reduced, and reelin immunoreactivity was barely detected (Fig. 5B, D, and F), in contrast to the localization of reelin immunoreactivity in the calretinin-positive neurons in superficial layer I of the wild-type mice (Fig. 5A, C, and E). Some of calretinin-immunopositive CR cells of the mutant neocortex appeared in a disorganized, scattered pattern other than the marginal zone (Fig. 5F). This finding was confirmed by in situ hybridization histochemistry of the neocortical primordium by using *reelin* cRNA probe as the marker for CR cells. The cells positive for *reelin* mRNA formed a thin superficial layer in wild-type mice (Fig. 6A and B). In contrast, the cells positive for *reelin* mRNA were scattered in the upper layer of the neocortical primordium of the mutant BiP mice (Fig. 6C and D). These findings of in situ hybridization histochemistry correspond well with those of calretinin-immunoreactive cells. Furthermore, the present findings indicate that the transcription of the *reelin* gene takes place to a similar degree in both mutant and wild-type mice, but the reelin protein is significantly reduced in the CR cells of the mutant.

While this mouse does have features of a *reeler* mutant phenotype, such as an outside-in pattern of neocortical layer formation and the migration defect of Purkinje cells in the cerebellum, it also has other phenotypes in the brain that are distinct from the *reeler* phenotype. These include the reduction in the size of the whole brain and the apparent scattering of reelin- and calretinin-positive neurons throughout the cortex. This is not surprising since BiP likely has a multitude of substrates that are significant for brain development. Among them, we decided to focus on reelin since at least one of the reeler mutants has a defect in intracellular transport of reelin (11) rather than the production of reelin, and the transport mutant BiP may affect the folding and secretion of reelin.

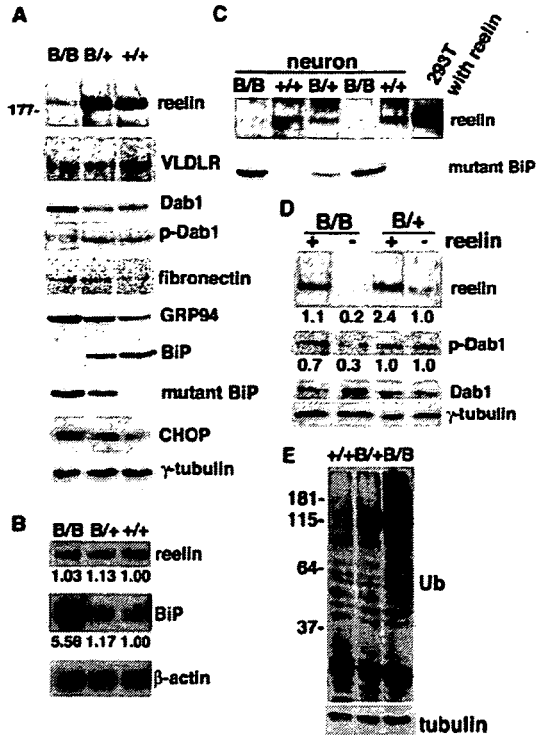

FIG. 7. Reelin expression is reduced posttranscriptionally in the mutant BiP brain. (A) The levels of expression of reelin, VLDLR, Dab1, tyrosine-phosphorylated Dab1 (p-Dab1), fibronectin, GRP94, BiP, mutant BiP, CHOP, and γ-tubulin in brains of E18.5 embryos were evaluated by Western blotting. In mutant BiP, the carboxyl-terminal KDEL sequence was replaced by an HA tag. (B) Northern blotting using probes for reelin, BiP, and β-actin mRNAs in brains at E18.5. The expression levels of reelin and BiP mRNAs were assessed by the relative ratio to β-actin mRNA. (C) Secretion of reelin and mutant BiP in the culture medium from the primary neurons and 293T cells transfected with reelin cDNA, as evaluated by Western blotting. (D) Primary neurons were treated with control (−) or reelin-containing medium (+) at 37°C for 20 min, collected, and subjected to Western blotting with antibodies against reelin, Dab1, tyrosine-phosphorylated Dab1, and γ-tubulin. The expression levels of reelin and tyrosine-phosphorylated Dab1 were assessed by the relative ratios to γ-tubulin. (E) Expression of ubiquitinated (Ub) proteins in the cerebrum at E18.5 embryos, as evaluated by Western blotting. B/B, homozygous mice; B/+, heterozygous mutant mice; +/+, wild-type mice.

Reelin secretion is impaired in the mutant BiP brain. Reelin is a large secreted glycoprotein (9) produced by some cortical neurons such as CR cells in the marginal zone during development. Reelin mediates cortical laminar formation through binding to VLDLR and apolipoprotein E receptor type 2 (ApoER2) on cortical neurons (8, 43). In *reeler* mice deficient in the reelin gene (9), the cortical neurons lack the ability to localize properly and settle inside the earlier-migrating neurons (7).

In E18.5 mice, we used an antibody directed against the amino terminus of reelin to detect a fragment of reelin (~180 kDa) in the wild-type cerebral cortex; however, these fragments were much less intense in the homozygous mutant BiP cortex (Fig. 7A), consistent with histological observations. Although VLDLR expression was equivalent between wild-type and mutant BiP cortices, dephosphorylated Dab1 accumulated in the mutant BiP brain, indicating that the reelin signaling pathway was inactivated there. The expression of another secreted glycoprotein, fibronectin, was preserved in the mutant brain. The reelin deficiency was not a consequence of reduced transcription, because *reelin* mRNA expression did not differ in control and mutant brains (Fig. 7B), consistent with the in situ hybridization experiment (Fig. 6). The expression of *BiP* mRNA as well as CHOP protein (a cell death-related transcriptional factor of the UPR) (50) was enhanced in the mutant brain (Fig. 7A and B), suggesting that the mutant brain suffered from ER stress.

Mutant BiP might impair the folding of reelin, leading to its degradation by the ER-associated degradation pathway or to its secretion as an immature form from the CR cells due to an escape from ER quality control. To test this possibility, we used primary neurons derived from embryonic brains and found a significant decrease in reelin secretion by the homozygous mutant BiP neurons compared with that of wild-type or heterozygous neurons (Fig. 7C). To investigate whether the homozygous mutant BiP neurons maintained their responsiveness to reelin stimulation, we incubated primary neurons with conditioned culture medium containing a severalfold physiological level of reelin secreted by 293T cells transiently transfected with reelin cDNA (Fig. 7D). Exogenous reelin seemed to be active on the homozygous neurons, leading to the activation of the reelin signaling pathway, as demonstrated by a reduced amount of Dab1 expression and an increased amount of phospho-Dab1 expression. On the other hand, the reelin signaling pathway in the heterozygous mutant cortical neurons seems to be constitutively active with endogenous reelin even without exogenous reelin stimulation. Thus, Dab1 expression and phosphorylation (Fig. 7D) are rather unchanged in the heterozygous mutant. These results suggest that the impaired secretion of reelin by the CR cells rather than defective responsiveness in the cortical neurons may be responsible for the neurological phenotype of *reeler* mutant-like malformations in mutant BiP mice. Thus, the impaired retrieval of BiP may promote the degradation of misfolded proteins by the ubiquitin/proteasome pathway. In fact, ubiquitinated proteins accumulated in the mutant cerebrum (Fig. 7E).

BiP may enhance the folding of reelin. Mutant BiP was detected in the ER (29), but a significant fraction was also secreted from cells because of the lack of the retrieval motif (KDEL) (Fig. 7C). We examined the subcellular localization of reelin to establish its relationship with mutant and wild-type BiP. Reelin colocalized with mutant BiP in the ER in primary neurons derived from heterozygous mutant BiP embryos; this was also the case in cortical neurons in the homozygous mutant postnatal brain, where the expression of reelin was reduced (Fig. 8A). To obtain further insight into the interaction of BiP and reelin, we performed cotransfection experiments in HeLa cells. Coexpression of reelin and wild-type BiP, but not the mutant BiP lacking the KDEL sequence, greatly enhanced the expression of reelin protein (reelin mRNA levels were equivalent in the two transfections) (Fig. 8B). These results suggest that BiP promotes the folding of reelin.

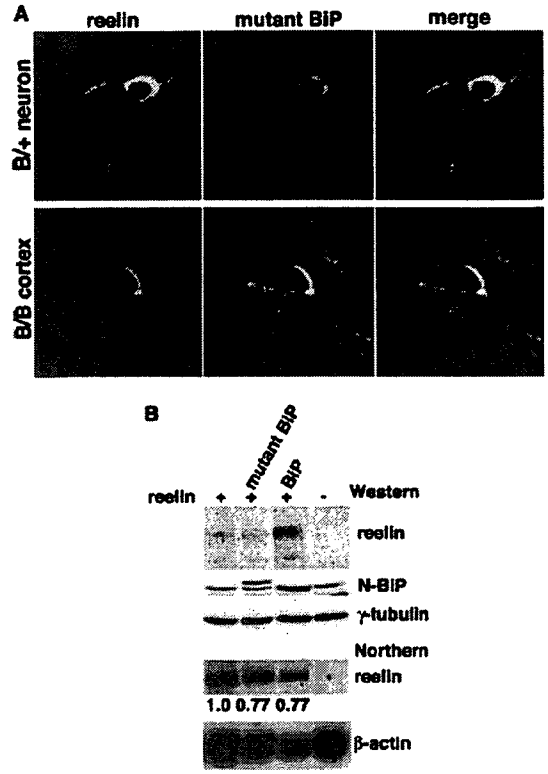

FIG. 8. BiP may enhance the maturation of reelin. (A) Subcellular localization of endogenous reelin and mutant BiP in primary neurons from the heterozygous (B/+) mutant BiP embryo and the cortex of the homozygous (B/B) mutant BiP embryo (E18.5), as evaluated by confocal laser scanning microscopy, with double labeling using a mouse mAb for reelin and a rabbit antiserum for HA. Scale bars, 10 μm. (B) HeLa cells were transiently transfected with reelin alone or co-transfected with either mutant BiP in which the KDEL sequence was replaced by a Myc tag or wild-type BiP (the Myc-tagged mutant BiP has a higher molecular weight than wild-type BiP). The levels of expression of reelin, BiP, and γ-tubulin were evaluated by Western blotting, and the levels of expression of *reelin* and β-*actin* mRNA were evaluated by Northern blotting. The expression level of *reelin* mRNA was assessed relative to that of β-*actin* mRNA.

DISCUSSION

We produced knock-in mice expressing a mutant BiP with the retrieval sequence deleted, which allowed us to examine the effects of a defect in the response to secretory pathway stress without completely eliminating BiP function, as would be the case with BiP knockout mice (28). The loss of BiP function was compensated for by the UPR in embryonic fibroblasts. However, neonates expressing mutant BiP suffered respiratory failure caused by the impaired secretion of pulmonary surfactant in alveolar type II epithelial cells (29). Furthermore, we observed abnormal corticogenesis in mutant BiP mice. Mutant BiP may predominantly affect dedicated secretory cells, such as alveolar type II cells and CR cells, in which active secretion is particularly important; thus, protein folding was probably affected in these cells. Indeed, we found an impaired secretion of reelin in CR cells, which may account for one aspect of cortical malformation in the cerebrum and cerebellum of mutant BiP mice. We also demonstrated increased Dab1 protein levels and a reduction in Dab1 tyrosine phosphorylation, which are consistent with a *reeler*-like phenotype. On the other hand, this mouse has other phenotypes in the brain that are distinct from the *reeler* phenotype. These include the reduction in the size of the whole brain and the apparent scattering of CR cells throughout the cortex, suggesting that mutant BiP may likely interfere with other substrates in addition to the reelin required for brain development.

The deletion of the retrieval sequence from BiP could have two possible effects. First, the lack of recycling of mutant BiP to the ER could impair the folding environment in the ER. This effect may be limited because constitutively active UPR compensates for it, and a sufficient amount of the functional mutant BiP, as long as it stays in the ER, may be produced for cell survival. Second, the impaired retrieval of mutant BiP may affect quality control in post-ER compartments. In addition to the ER itself, several studies have revealed that proper ER-to-Golgi apparatus transport and the subsequent retrieval/return of proteins and lipids to the ER may contribute to quality control (16, 19, 42, 45, 47). In this regard, the folding (and therefore function) of reelin may be dependent on the proper retrieval of BiP to the ER via interactions with the KDEL receptor.

Reelin is a large 3,461-residue secreted glycoprotein that has eight reelin repeats of ~350 residues each that contain an epidermal growth factor motif followed by a carboxyl-terminal 33 residues rich in basic amino acids (43). During embryogenesis, CR cells secrete reelin as homo-oligomers that function in cortical layer formation through binding to lipoprotein receptors on cortical neurons (44). Although the folding, intracellular transport, and oligomerization of reelin have not been characterized in detail, we found that reelin protein expression was impaired in mutant BiP mice, indicating that BiP may play a role in the maturation of reelin. Furthermore, we found that the expression levels of BiP mRNA and the CHOP protein were enhanced in the mutant brain, suggesting that the mutant brain might have suffered from ER stress. We speculate that the folding of the reelin protein may be vulnerable to impaired quality control in the ER and the post-ER compartments of mutant CR cells. If true, this assumption suggests that environmental stresses that perturb ER quality control may also impair the reelin signaling pathway and other factors, which may cause neuronal migration defects.

In addition to brain development, several studies suggested the possible role of reelin in the pathogenesis of human mental disorders such as schizophrenia, autism, bipolar disorder, and Alzheimer's disease (5, 14, 43). Because reelin signaling through ApoER2 in adult brains modulates synaptic plasticity and memory formation (2), the defective reelin signaling pathway may contribute to the pathogenesis of adult mental disorders. Reelin and ApoE share ApoER2 on cortical neurons (8), and ApoE inhibits reelin signaling by competing for binding to ApoER2. Interestingly, the E4 allele of ApoE increases the risk of developing sporadic forms of Alzheimer's disease.

In the meantime, the persistent accumulation of misfolded proteins beyond the capacity of ER quality control causes ER stress, leading to cellular dysfunction and cell death (24, 26). This process is thought to cause human mental disorders such as neurodegenerative diseases including Alzheimer's disease (23) and Parkinson's disease (21), bipolar disorders (22), and

ischemic neuronal injury (41). The involvement of impaired BiP function in neurodegenerative diseases has been reported in a mouse model where the disruption of SIL1, a cochaperone of BiP, caused protein accumulation and neurodegeneration (49). Thus, reelin signaling and ER quality control may be related to the pathogenesis of adult mental disorders, as seen in reeler mutant-like cerebral malformation in mutant BiP neonates.

The UPR is a ubiquitous mechanism in all cells to adapt to ER stress in pathological conditions, and BiP is an essential component of this system. Our results suggest that a physiological increase in the production of reelin and other factors in dedicated secretory cells like CR cells during neonatal periods may require the UPR and a proper folding capacity in the ER. Neuronal migration and stratification may be sensitive to environmental insults such as viral infection, hypoxia, and ischemia that perturb ER functions.

ACKNOWLEDGMENTS

We thank T. Nishino, K. Toshimori, and T. Yamashita for critical comments. We also thank M. Kashio for excellent technical assistance.

This work was supported by grants-in-aid for science research from the Ministry of Education, Culture, Sports, Science, and Technology of Japan to T.A. and grant 05-32 from NIBIO to S.Y.

REFERENCES

1. **Banker, G., and K. Goslin.** 1988. Developments in neuronal cell culture. Nature **336**:185–186.
2. **Beffert, U., E. J. Weeber, A. Durudas, S. Qiu, I. Masiulis, J. D. Sweatt, W. P. Li, G. Adelmann, M. Frotscher, R. E. Hammer, and J. Herz.** 2005. Modulation of synaptic plasticity and memory by Reelin involves differential splicing of the lipoprotein receptor Apoer2. Neuron **47**:567–579.
3. **Beh, C. T., and M. D. Rose.** 1995. Two redundant systems maintain levels of resident proteins within the yeast endoplasmic reticulum. Proc. Natl. Acad. Sci. USA **92**:9820–9823.
4. **Bonifacino, J. S., and A. M. Weissman.** 1998. Ubiquitin and the control of protein fate in the secretory and endocytic pathways. Annu. Rev. Cell Dev. Biol. **14**:19–57.
5. **Bothwell, M., and E. Giniger.** 2000. Alzheimer's disease: neurodevelopment converges with neurodegeneration. Cell **102**:271–273.
6. **Brodsky, J. L., and A. A. McCracken.** 1999. ER protein quality control and proteasome-mediated protein degradation. Semin. Cell Dev. Biol. **10**:507–513.
7. **Caviness, V. S., Jr.** 1982. Neocortical histogenesis in normal and reeler mice: a developmental study based upon [3H]thymidine autoradiography. Brain Res. **256**:293–302.
8. **D'Arcangelo, G., R. Homayouni, L. Keshvara, D. S. Rice, M. Sheldon, and T. Curran.** 1999. Reelin is a ligand for lipoprotein receptors. Neuron **24**:471–479.
9. **D'Arcangelo, G., G. G. Miao, S. C. Chen, H. D. Soares, J. I. Morgan, and T. Curran.** 1995. A protein related to extracellular matrix proteins deleted in the mouse mutant *reeler*. Nature **374**:719–723.
10. **D'Arcangelo, G., K. Nakajima, T. Miyata, M. Ogawa, K. Mikoshiba, and T. Curran.** 1997. Reelin is a secreted glycoprotein recognized by the CR-50 monoclonal antibody. J. Neurosci. **17**:23–31.
11. **de Bergeyck, V., K. Nakajima, C. Lambert de Rouvroit, B. Naerhuyzen, A. M. Goffinet, T. Miyata, M. Ogawa, and K. Mikoshiba.** 1997. A truncated Reelin protein is produced but not secreted in the 'Orleans' reeler mutation (Reln[rl-Orl]). Brain Res. Mol. Brain Res. **50**:85–90.
12. **Ellgaard, L., and A. Helenius.** 2003. Quality control in the endoplasmic reticulum. Nat. Rev. Mol. Cell Biol. **4**:181–191.
13. **Falconer, D. S.** 1951. Two new mutant, 'trembler' and 'reeler,' with neurological actions in the house mouse (Mus muscululus L.). J. Genet. **50**:192–201.
14. **Fatemi, S. H.** 2005. Reelin glycoprotein: structure, biology and roles in health and disease. Mol. Psych. **10**:251–257.
15. **Hamada, H., M. Suzuki, S. Yuasa, N. Mimura, N. Shinozuka, Y. Takada, T. Nishino, H. Nakaya, H. Koseki, and T. Aoe.** 2004. Dilated cardiomyopathy caused by aberrant endoplasmic reticulum quality control in mutant KDEL receptor transgenic mice. Mol. Cell. Biol. **24**:8007–8017.
16. **Hammond, C., and A. Helenius.** 1994. Quality control in the secretory pathway: retention of a misfolded viral membrane glycoprotein involves cycling between the ER, intermediate compartment, and Golgi apparatus. J. Cell Biol. **126**:41–52.
17. **Harding, H. P., and D. Ron.** 2002. Endoplasmic reticulum stress and the development of diabetes: a review. Diabetes **51**(Suppl. 3):S455–S461.
18. **Harding, H. P., Y. Zhang, and D. Ron.** 1999. Protein translation and folding are coupled by an endoplasmic-reticulum-resident kinase. Nature **397**:271–274.
19. **Haynes, C. M., S. Caldwell, and A. A. Cooper.** 2002. An HRD/DER-independent ER quality control mechanism involves Rsp5p-dependent ubiquitination and ER-Golgi transport. J. Cell Biol. **158**:91–101.
20. **Hsu, V. W., N. Shah, and R. D. Klausner.** 1992. A brefeldin A-like phenotype is induced by the overexpression of a human ERD-2-like protein, ELP-1. Cell **69**:625–635.
21. **Imai, Y., M. Soda, H. Inoue, N. Hattori, Y. Mizuno, and R. Takahashi.** 2001. An unfolded putative transmembrane polypeptide, which can lead to endoplasmic reticulum stress, is a substrate of Parkin. Cell **105**:891–902.
22. **Kakiuchi, C., K. Iwamoto, M. Ishiwata, M. Bundo, T. Kasahara, I. Kusumi, T. Tsujita, Y. Okazaki, S. Nanko, H. Kunugi, T. Sasaki, and T. Kato.** 2003. Impaired feedback regulation of XBP1 as a genetic risk factor for bipolar disorder. Nat. Genet. **35**:171–175.
23. **Katayama, T., K. Imaizumi, N. Sato, K. Miyoshi, T. Kudo, J. Hitomi, T. Morihara, T. Yoneda, F. Gomi, Y. Mori, Y. Nakano, J. Takeda, T. Tsuda, Y. Itoyama, O. Murayama, A. Takashima, P. St. George-Hyslop, M. Takeda, and M. Tohyama.** 1999. Presenilin-1 mutations downregulate the signalling pathway of the unfolded-protein response. Nat. Cell Biol. **1**:479–485.
24. **Kaufman, R. J.** 2002. Orchestrating the unfolded protein response in health and disease. J. Clin. Investig. **110**:1389–1398.
25. **Kleizen, B., and I. Braakman.** 2004. Protein folding and quality control in the endoplasmic reticulum. Curr. Opin. Cell Biol. **16**:343–349.
26. **Kopito, R. R., and D. Ron.** 2000. Conformational disease. Nat. Cell Biol. **2**:E207–E209.
27. **Lewis, M. J., and H. R. Pelham.** 1990. A human homologue of the yeast HDEL receptor. Nature **348**:162–163.
28. **Luo, S., C. Mao, B. Lee, and A. S. Lee.** 2006. GRP78/BiP is required for cell proliferation and protecting the inner cell mass from apoptosis during early mouse embryonic development. Mol. Cell. Biol. **26**:5688–5697.
29. **Mimura, N., H. Hamada, M. Kashio, H. Jin, Y. Toyama, K. Kimura, M. Iida, S. Goto, H. Saisho, K. Toshimori, H. Koseki, and T. Aoe.** 2007. Aberrant quality control in the endoplasmic reticulum impairs the biosynthesis of pulmonary surfactant in mice expressing mutant BiP. Cell Death Differ. **14**:1475–1485.
30. **Munro, S., and H. R. Pelham.** 1987. A C-terminal signal prevents secretion of luminal ER proteins. Cell **48**:899–907.
31. **Munro, S., and H. R. Pelham.** 1986. An Hsp70-like protein in the ER: identity with the 78 kd glucose-regulated protein and immunoglobulin heavy chain binding protein. Cell **46**:291–300.
32. **Ogawa, M., T. Miyata, K. Nakajima, K. Yagyu, M. Seike, K. Ikenaka, H. Yamamoto, and K. Mikoshiba.** 1995. The reeler gene-associated antigen on Cajal-Retzius neurons is a crucial molecule for laminar organization of cortical neurons. Neuron **14**:899–912.
33. **Ohshima, T., J. M. Ward, C. G. Huh, G. Longenecker, Veeranna, H. C. Pant, R. O. Brady, L. J. Martin, and A. B. Kulkarni.** 1996. Targeted disruption of the cyclin-dependent kinase 5 gene results in abnormal corticogenesis, neuronal pathology and perinatal death. Proc. Natl. Acad. Sci. USA **93**:11173–11178.
34. **Oyadomari, S., A. Koizumi, K. Takeda, T. Gotoh, S. Akira, E. Araki, and M. Mori.** 2002. Targeted disruption of the Chop gene delays endoplasmic reticulum stress-mediated diabetes. J. Clin. Investig. **109**:525–532.
35. **Patil, C., and P. Walter.** 2001. Intracellular signaling from the endoplasmic reticulum to the nucleus: the unfolded protein response in yeast and mammals. Curr. Opin. Cell Biol. **13**:349–355.
36. **Reimold, A. M., A. Etkin, I. Clauss, A. Perkins, D. S. Friend, J. Zhang, H. F. Horton, A. Scott, S. H. Orkin, M. C. Byrne, M. J. Grusby, and L. H. Glimcher.** 2000. An essential role in liver development for transcription factor XBP-1. Genes Dev. **14**:152–157.
37. **Reimold, A. M., N. N. Iwakoshi, J. Manis, P. Vallabhajosyula, E. Szomolanyi-Tsuda, E. M. Gravallese, D. Friend, M. J. Grusby, F. Alt, and L. H. Glimcher.** 2001. Plasma cell differentiation requires the transcription factor XBP-1. Nature **412**:300–307.
38. **Scheuner, D., B. Song, E. McEwen, C. Liu, R. Laybutt, P. Gillespie, T. Saunders, S. Bonner-Weir, and R. J. Kaufman.** 2001. Translational control is required for the unfolded protein response and in vivo glucose homeostasis. Mol. Cell **7**:1165–1176.
39. **Schroder, M., and R. J. Kaufman.** 2005. The mammalian unfolded protein response. Annu. Rev. Biochem. **74**:739–789.
40. **Sonnichsen, B., J. Fullekrug, P. N. Van, W. Diekmann, D. G. Robinson, and G. Mieskes.** 1994. Retention and retrieval: both mechanisms cooperate to maintain calreticulin in the endoplasmic reticulum. J. Cell Sci. **107**:2705–2717.
41. **Tajiri, S., S. Oyadomari, S. Yano, M. Morioka, T. Gotoh, J. I. Hamada, Y. Ushio, and M. Mori.** 2004. Ischemia-induced neuronal cell death is mediated by the endoplasmic reticulum stress pathway involving CHOP. Cell Death Differ. **11**:403–415.

42. **Taxis, C., F. Vogel, and D. H. Wolf.** 2002. ER-Golgi traffic is a prerequisite for efficient ER degradation. Mol. Biol. Cell **13**:1806–1818.
43. **Tissir, F., and A. M. Goffinet.** 2003. Reelin and brain development. Nat. Rev. Neurosci. **4**:496–505.
44. **Utsunomiya-Tate, N., K. Kubo, S. Tate, M. Kainosho, E. Katayama, K. Nakajima, and K. Mikoshiba.** 2000. Reelin molecules assemble together to form a large protein complex, which is inhibited by the function-blocking CR-50 antibody. Proc. Natl. Acad. Sci. USA **97**:9729–9734.
45. **Vashist, S., and D. T. Ng.** 2004. Misfolded proteins are sorted by a sequential checkpoint mechanism of ER quality control. J. Cell Biol. **165**:41–52.
46. **Wu, J., and R. J. Kaufman.** 2006. From acute ER stress to physiological roles of the unfolded protein response. Cell Death Differ. **13**:374–384.
47. **Yamamoto, K., R. Fujii, Y. Toyofuku, T. Saito, H. Koseki, V. W. Hsu, and T. Aoe.** 2001. The KDEL receptor mediates a retrieval mechanism that contributes to quality control at the endoplasmic reticulum. EMBO J. **20**:3082–3091.
48. **Yuasa, S., J. Kitoh, S. Oda, and K. Kawamura.** 1993. Obstructed migration of Purkinje cells in the developing cerebellum of the reeler mutant mouse. Anat. Embryol. (Berlin) **188**:317–329.
49. **Zhao, L., C. Longo-Guess, B. S. Harris, J. W. Lee, and S. L. Ackerman.** 2005. Protein accumulation and neurodegeneration in the woozy mutant mouse is caused by disruption of SIL1, a cochaperone of BiP. Nat. Genet. **37**:974–979.
50. **Zinszner, H., M. Kuroda, X. Wang, N. Batchvarova, R. T. Lightfoot, H. Remotti, J. L. Stevens, and D. Ron.** 1998. CHOP is implicated in programmed cell death in response to impaired function of the endoplasmic reticulum. Genes Dev. **12**:982–995.

Available online at www.sciencedirect.com
ScienceDirect
European Journal of Pharmacology 573 (2007) 20–28
www.elsevier.com/locate/ejphar

Alpha 1-adrenoceptor agonists protect against stress-induced death of neural progenitor cells

Hiroki Ohashi [a,b], Kaori Nishikawa [a,c], Koichi Ayukawa [a,d], Yoko Hara [a], Mika Nishimoto [a,e], Yoshihisa Kudo [e], Toshiaki Abe [b], Shunsuke Aoki [a,c,f,*], Keiji Wada [a,f]

[a] *Department of Degenerative Neurological Diseases, National Institute of Neuroscience, NCNP, Kodaira, Tokyo 187-8502, Japan*
[b] *Department of Neurosurgery, Jikei University Graduate School of Medicine, Minatoku, Tokyo 105-8401, Japan*
[c] *NEDO (New Energy and Industrial Technology Development Organization), Kawasaki, Kanagawa 212-8554, Japan*
[d] *Japan Society for the Promotion of Science (JSPS), Chiyodaku, Tokyo 102-8471, Japan*
[e] *Laboratory of Cellular Neurobiology, Tokyo University of Pharmacy and Life Science, Hachioji, Tokyo 192-0392, Japan*
[f] *CREST (Core Research for Evolutional Science and Technology) of Japan Science and Technology Corporation (JST), Kawaguchi, Saitama 332-0012, Japan*

Received 15 February 2007; received in revised form 18 June 2007; accepted 26 June 2007
Available online 12 July 2007

Abstract

Here, we show that α_1-adrenoceptor agonists suppress stress-induced death of mouse embryonic brain-derived neural progenitor cells (NPCs). NPCs highly expressed both α_{1A}- and α_{1B}-adrenoceptor genes, whereas the gene encoding α_{1D}-adrenoceptor was expressed at low levels. Application of the α_1-adrenoceptor agonists phenylephrine and cirazoline significantly promoted cell survival of embryonic NPCs that had been exposed to stress, as measured by a lactate dehydrogenase release assay, but had no remarkable effect on differentiation of the NPCs. Both phenylephrine and cirazoline protected NPCs from death induced by growth factor deprivation, N2 nutrient deprivation, tunicamycin treatment or staurosporine treatment. Phenylephrine and cirazoline treatments both maximally reduced stress-induced cell death by ~60% but did not change the percentage of undifferentiated cells as measured by nestin staining. Moreover, phenylephrine and cirazoline treatments did not affect the cellular activities of caspase-3 and caspase-7 but markedly reduced propidium iodide penetration into the cytoplasm, suggesting that α_1-adrenoceptor agonists inhibit caspase-3/7-independent death of the embryonic NPCs.

Keywords: α_1-adrenoceptor; GPCR; Neural progenitor cell; Cell death; Cell stress; Phenylephrine; Cirazoline

1. Introduction

The noradrenergic system is proposed to play multiple roles in the adult central nervous system (CNS). Apart from its classical transmitter signaling action, noradrenaline has important roles in attention, arousal, and memory reviewed in Murchison et al., (2004); Southwick et al., (1999). Furthermore, it was proposed that noradrenaline influences the survival, maintenance and plasticity of CNS neurons, including the regulation of endogenous neurotrophin systems, glial function, CNS energy utilization and extracellular homeostasis, and has anti-inflammatory and anti-oxidant effects reviewed in Marien et al., (2004). All cell surface adrenoceptors are members of the G protein-coupled receptor family and mediate responses to extracellular noradrenaline. To date, three subfamilies of adrenoceptors (α_1, α_2 and β) have been identified (Bylund et al., 1995). The adrenoceptors are expressed in many tissues, particularly in the cardiovascular, genitourinary and nervous systems. High levels of adrenoceptors are also present in the neocortex during embryogenesis (Lidow and Rakic, 1992), and there are regional concentrations of α_1, α_2, and β adrenoceptors in the fetal forebrain (Lidow and Rakic, 1994). There are three subtypes of α_1-adrenoceptors, the α_{1A}, α_{1B}, α_{1D}-adrenoceptor, with varying degrees of efficiency of G protein (Gq/11) coupling ($\alpha_{1A} > \alpha_{1B} > \alpha_{1D}$ adrenoceptor) reviewed in Hieble et al., (1995). This leads to activation of downstream signal

* Corresponding author. Department of Degenerative Neurological Diseases, National Institute of Neuroscience, National Center of Neurology and Psychiatry, 4-1-1 Ogawahigashi, Kodaira, Tokyo 187-8502, Japan. Tel.: +81 42 346 1715; fax: +81 42 346 1745.
E-mail address: aokis@ncnp.go.jp (S. Aoki).

0014-2999/$ - see front matter © 2007 Elsevier B.V. All rights reserved.
doi:10.1016/j.ejphar.2007.06.060

transduction pathways, including Ca^{2+}, arachidonic acid, phospholipase C and phospholipase D signals reviewed in Zhong and Minneman (1999). α_1-adrenoceptors are specifically localized to NPCs located in the ventricular zone and subventricular zone in the embryonic rat forebrain, and noradrenaline-containing fibers are also present in both the ventricular zone and subventricular zone (Pabbathi et al., 1997). In addition, noradrenaline has been suggested to regulate development of the murine forebrain. The β-adrenoceptor agonist isoproterenol alters proliferation and differentiation of neural precursors in the cerebral cortex (Slotkin et al., 1988). α_1-adrenoceptors were also implicated in controlling cell proliferation and survival in a rat cortical mixed cell culture and in a heterochronic coculture system of the rat neocortex and rostral pons (Pabbathi et al., 1997; Popovik and Haynes, 2000). Although the functions of α_1-adrenoceptors in the mixed-culture NPCs and in the organ culture were investigated, the function of α_1-adrenoceptors and the direct effects of α_1-adrenoceptor-selective agonists such as phenylephrine and cirazoline in isolated pure embryonic NPCs are not known.

The precise role of the α_1-adrenoceptor-mediated signal in embryonic cortical NPCs remains obscure, because the effects observed in the mixed-cell and organ culture experiments possibly reflect the secondary and tertiary effects mediated by multiple cellular interactions (glial cell-progenitor, neuronal cell-progenitor and neuronal cell-glial cell-progenitor interactions). As such, the aim of this study is to know the primary biological effect of α_1-adrenoceptor activation in the NPCs. We addressed the biological effects of α_1-adrenoceptor-selective agonists on highly purified embryonic NPCs. Our data indicate that these agonists inhibit death of NPCs cultured under various stress conditions but do not affect proliferation, differentiation or caspase-3/7-activity.

2. Materials and methods

2.1. Animals

Pregnant C57BL/6J mice were purchased from CLEA Japan (Tokyo, Japan). Animal care and handling were in accordance with institutional regulations for animal care and public law, and were approved by the Animal Investigation Committee of the National Institute of Neuroscience, Japan.

2.2. Antibodies and reagents

Monoclonal and polyclonal antibodies used in this study were as follows: monoclonal anti-nestin (Becton Dickinson, Lexington, KY), monoclonal anti-tuj1 (Covance, Berkeley, CA), polyclonal anti-glial fibrillary acidic protein (Dako, Carpinteria, CA), monoclonal anti-galactocerebroside (Chemicon International, Temecula, CA). The secondary antibodies conjugated to Alexa Fluor dye were purchased from Molecular Probes (Eugene, OR). α_1-adrenoceptor agonists used in this study were (*R*)-3-[1-hydroxy-2-(methylamino) ethyl] phenol (phenylephrine; Sigma, St. Louis, MO) and 2-[(2-cyclopropyl-phenoxy) methyl]-4, 5-dihydro-1H-imidazole (cirazoline; Tocris, Ellisville, MO). Each agonist was dissolved in Neurobasal™ medium (Invitrogen, Carlsbad, CA). Staurosporine and tunicamycin (Sigma) were dissolved in dimethyl sulfoxide (DMSO). Each solution was added to the medium, and the final concentration of DMSO in the medium was adjusted to at most 0.1% (v/v). Medium containing the same amount of organic solvent was used as a negative control.

2.3. Cortical NPCs culture

Cortical NPCs were cultured as previously described (Fukazawa et al., 2006). Briefly, embryos were removed from pregnant C57BL/6J mice and were staged according to morphological criteria to confirm gestational age. Developing mouse brain and cerebral cortex containing the ventricular and subventricular zones were dissected from embryonic day 14 (E14) embryos. Cells were mechanically dissociated by trituration and plated at 3.0×10^6 cells per 10-cm dish (BD) precoated with 15 μg/ml poly-L-ornithine (Sigma) and 1 μg/ml fibronectin (Nitta Gelatin, Osaka, Japan). Cells were expanded for 4 days in serum-free Neurobasal medium supplemented with 0.5 mM L-glutamine (Invitrogen), 100 U/ml penicillin, 100 μg/ml streptomycin (Invitrogen) and B27 (biotin, L-carnitine, corticosterone, ethanolamine, D(+)-galactose, glutathione (reduced), linoleic acid, linolenic acid, progesterone, putrescine, retinyl acetate, selenium, T3 (triodo-l-thyronine), DL-α-tocopherol (vitamin E), DL-α-tocopherol acetate, bovine serum albumin, catalase, insulin, superoxide dismutase, transferrin, vitamin A (Brewer et al., 1993); Invitrogen). N2 supplement (100 mg/l apo-transferrin, 5 mg/l insulin, 16 mg/l putrescine, 6.3 μg/l progesterone, 5 μg/l selenite; Sigma) were used for stress experiments instead of the B27 supplement. This medium was supplemented with 10 ng/ml basic fibroblast growth factor (bFGF; PeproTech, Rocky Hill, NJ) except when mentioned otherwise. Cultures were maintained at 37 °C in an atmosphere of 95% air and 5% CO_2. For secondary cultures, bFGF-expanded cortical NPCs were washed in warm Hanks' balanced salt solution, detached with mechanically pipetting, and resuspended in Neurobasal medium. Cells were then re-seeded on 24-well plates (Nunc; 1.8×10^5 cells/well), or 48-well plates (Nunc; 1.5×10^5 cells/well) precoated with poly-L-ornithine and fibronectin.

2.4. Real-time quantitative reverse-transcription (RT)-PCR

Real-time quantitative RT-PCR with the SYBR Green-based detection method was performed as previously described (Aoki et al., 2002). Total RNA was isolated from cultured cortical NPCs and E14 mouse cerebral cortex. These RNAs (1 μg) were treated with DNase I and converted to cDNA with Superscript II reverse transcriptase (Invitrogen) and random hexamer primers according to the manufacturer's instructions. The efficiency of reverse transcription and the quality of cDNA was compared with the efficiency of PCR amplification of the hypoxanthine guanine phosphoribosyl transferase (hprt) gene (GenBank accession ID. NM_013556; forward primer, 5′-TCTTTGCTGACCTGCTG-GATT-3′; reverse primer, 5′-TATGTCCCCCGTTGACTGATC-

3′). Primers were designed for the α_{1A} (NM_013461), α_{1B} (NM_007416) and α_{1D} (NM_013460) adrenoceptor genes using Primer Express software (Perkin-Elmer, Torrance, CA). The forward and reverse primer sequences were as follows: 5′-TTTCAAGCCACCGGAAACA-3′ and 5′-ACTGGATTCGCAGCACATTCT-3′ (α_{1A}); 5′-AACCCTTCTACGCCCTCTTTTC-3′ and 5′-CCAGATTCTTGGTGGTCCTCTT-3′ (α_{1B}); and 5′-TCGCTCAAGTATCCAGCCATT-3′ and 5′-AACCTAGTAGCGGTCCCACAGA-3′ (α_{1D}). SYBR Green-based real-time RT-PCR was performed in 12.5-μl reactions (ABI PRISM 7700 Sequence Detection System, Perkin-Elmer). PCR products were analyzed with agarose gel electrophoresis. We checked each primer individually to ensure that the primer was selective for the target (data not shown). We also ensured that no band was observed in gel electrophoresis of PCRs that included distilled water or total RNA preparation without reverse transcriptase as template. The quantitative RT-PCR method (User Bulletin #2, Applied Biosystems, Foster City, CA) was modified to establish an expression level index for mRNA (Aoki et al., 2002), and the SYBR Green signal for the hprt amplicon was used as a reference. Amplification efficiency was determined and confirmed in a control PCR experiment using serial cDNA dilutions as templates. The real-time RT-PCR products were analyzed using the Applied Biosystems sequence detection system software 1.7.

2.5. LDH and ATP assay

The number of non-viable cortical NPCs was quantitatively assayed by measuring the activity of the cytosolic enzyme lactate dehydrogenase (LDH) released into the culture medium after membrane rupture. LDH activity was measured using the cytotoxicity assay CytoTox-ONE™ Homogeneous Membrane Integrity Assay (Promega, Madison, WI). To quantify the number of viable cells in cultured cortical NPCs, the amount of cellular ATP was measured using the CellTiter-Glo™ Luminescent Cell Viability Assay (Promega). These assays were performed in accordance with the manufacturer's protocol and on secondary cultured cortical NPCs as described above. Four hundred μl (1.5×10^5 cells/well) of cell suspension was added to each well of a 48-well plate (Nunc) precoated with poly-L-ornithine and fibronectin. After 24 h, cells were treated without or with 10 μM phenylephrine or cirazoline with different concentrations of bFGF or under different stress conditions as described in the figure legends. Cultures were then returned to the 37 °C incubator for 24 h, and assessment of LDH release in the media and amount of ATP was conducted with a Wallac 1420 multilabel counter (Perkin-Elmer, Finland).

2.6. Immunocytochemistry

Cells were stained as we have previously described with minor modifications (Sakurai et al., 2006). Briefly, all incubations and washes were performed at room temperature. Cells were fixed with 3.8% formaldehyde in phosphate-buffered saline (PBS) for 10 min and permeabilized with 0.02% (w/v) Triton X-100 in PBS for 5 min. Fixed cells were blocked with 3.3% goat serum in PBS for 30 min. Cells were incubated for 30 min with anti-nestin (neural progenitor marker; 1:500), anti-tuj1 (early neuronal cell marker; 1:500)(Sakurai et al., 2006), anti-glial fibrillary acidic protein (astrocyte marker; 1:1000) or anti-galactocerebroside (immature oligodendrocyte marker; 1:200)(Fukazawa et al., 2006). These cells were incubated with diluted secondary antibody (1:200) conjugated to Alexa Fluor for 30 min. All primary and secondary antibodies were diluted in 1% goat serum in PBS before use. The fluorescence microscopy images were obtained with an IX70 microscope (Olympus).

2.7. Quantification of enzymatic activities of caspases

Caspase-3 and caspase-7 protease activities were determined using the Caspase-Glo™ 3/7 Assay kit (Promega). All assays were performed on secondary cultured cortical NPCs as described above. Four hundred μl (1.5×10^5 cells/well) of cell suspension was added to each well of a 48-well plate (Nunc) precoated with poly-L-ornithine and fibronectin. After 24 h, cells were treated with or without 10 μM phenylephrine in medium lacking the N2 supplement as described in the figure legends. Cultures were then returned to the 37 °C incubator for 24 h, and caspase-3 and -7 activities were assessed with a Wallac 1420 multilabel counter.

2.8. Measurement of cell death using propidium iodide

All assays were performed on secondary cultured cortical NPCs as described above. Four hundred μl (1.5×10^5 cells/well) of cell suspension was added to each well of a 48-well plate (Nunc) precoated with poly-L-ornithine and fibronectin. After 24 h, cells were treated with or without 10 μM phenylephrine in medium lacking the N2 supplement. Cultures were then returned to the 37 °C incubator and maintained for 24 h, then stained with 1 μg/ml propidium iodide. Only dead cells with permeable plasma membranes were stained with propidium iodide. Positive controls were stained with propidium iodide after fixing with 3.8% formaldehyde in PBS for 10 min and permeabilized with 0.02% Triton X-100 in PBS. Dead cells and positive controls stained with propidium iodide were counted by fluorometry (Wallac 1420 multilabel counter).

2.9. Statistical analysis

Results are expressed as the mean±standard error of the mean (S.E.M.). Either the Student's *t*-test or Dunnett's multiple range test was used to evaluate the data using Prism software version 4.03 (GraphPad, San Diego, CA). Values of $P<0.01$ and $P<0.05$ were considered statistically significant depending on the specific experiment.

3. Results

3.1. Embryonic cortical NPCs express α_1-adrenoceptor genes

We analyzed gene expression levels of the three α_1-adrenoceptors, and all were expressed both in the E14 embryonic

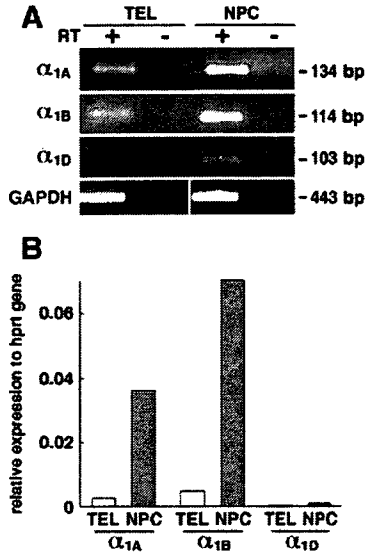

Fig. 1. NPCs derived from E14 telencephalon express α_{1A}-adrenoceptor (α_{1A}), α_{1B}-adrenoceptor (α_{1B}) and α_{1D}-adrenoceptor (α_{1D}). Total RNA isolated from cultured NPCs and E14 mouse telencephalon (TEL) was reverse-transcribed, and the resultant cDNA was used in RT-PCR analysis. (A) As indicated on the left, the PCR products corresponding to the α_{1A}, α_{1B}, and α_{1D} adrenoceptor genes and *GAPDH* were separated on a 3% agarose gel. The size of PCR products are indicated on the right. (B) Gene expression levels of the α_{1A}, α_{1B} and α_{1D} adrenoceptor were analyzed by quantitative RT-PCR, and the expression levels relative to *hprt* are presented. The results are representative of three separate experiments that yielded similar results.

telencephalon and E14 telencephalon-derived cultured NPCs (Fig. 1A). Semi-quantitative analysis of expression levels of the α_1-adrenoceptor genes (normalized to the internal control, *hprt*) showed that the isolated NPCs highly expressed α_{1A}, α_{1B} and α_{1D} adrenoceptor genes as compared with the E14 telencephalon (Fig. 1B). Among the α_1-adrenoceptor genes, the α_{1A} and α_{1B} genes were highly expressed in the cultured NPCs, whereas a low level of expression was detected for the α_{1D} gene in both the E14 telencephalon and cultured NPCs (Fig. 1B).

3.2. Effect of the α_1-adrenoceptor agonist phenylephrine on NPC differentiation

E14 telencephalon-derived NPCs have potencies to differentiate into multiple neural cell types, including neurons, astrocytes and oligodendrocytes, in the absence of bFGF (Fig. 2). The effect of phenylephrine, an α_1-adrenoceptor-selective agonist, on NPC differentiation was examined using the neural cell differentiation marker tuj1 for neuronal cells, glial fibrillary acidic protein for astroglial cells and galactocerebroside for oligodendrocytes. At 72 h after bFGF deprivation, 41.8±1.0% of the NPCs had differentiated into tuj1-positive (tuj1$^+$) cells, 40.6±6.0% of the NPCs had differentiated into glial fibrillary acidic protein-positive (GFAP$^+$) cells and 9.4±1.1% were galactocerebroside-positive (GC$^+$) (Fig. 2A and B). Phenylephrine treatment did not significantly change the percentages of neuronal and glial cells (tuj1$^+$, 38.1±3.2%; GFAP$^+$, 28.7±3.1%; and GC$^+$, 6.2±1.0%) in cultures lacking bFGF (Fig. 2A and B). These results indicate that phenylephrine did not affect NPC differentiation induced by bFGF deprivation. We also examined the effect of phenylephrine on neural differentiation of NPCs in cultures containing bFGF and again found no effect on neuronal or glial differentiation (data not shown).

3.3. α_1-adrenoceptor agonists protect NPCs from cell death

It has been reported that activation of α_1-adrenoceptors stimulates DNA synthesis of embryonic NPCs in mixed culture conditions (Pabbathi et al., 1997). Primary NPC cultures prepared from the telencephalon contain a considerable number of neuronal cells (>10%) that also express α_1-adrenoceptors (Papay et al., 2006). To determine whether the previously reported activation of DNA synthesis was indicative of NPC proliferation or proliferation by secondary effect via other cell types contaminating the culture, we re-seeded cultured NPCs from a primary culture to prepare highly purified secondary

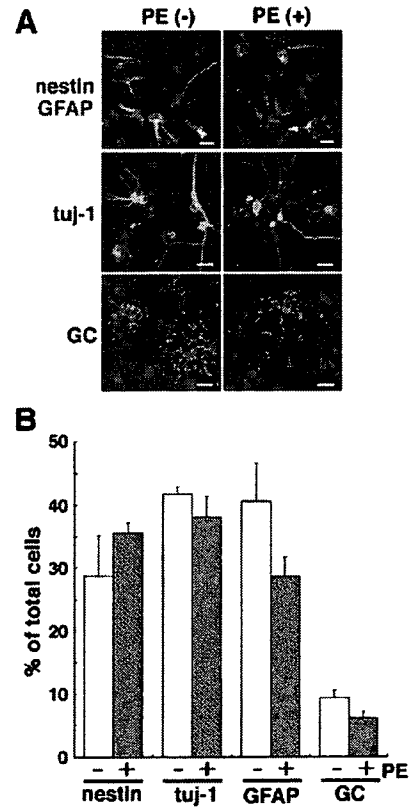

Fig. 2. Effect of the α_1-adrenoceptor agonist phenylephrine on NPC differentiation. (A) Immunofluorescence staining was carried out after 72 h on NPC cultures with or without phenylephrine. Fluorescence microscopic images of cells labeled with anti-nestin (green), anti-GFAP (red), anti-tuj1 (green) and anti-galactocerebroside (green) are shown; nuclei are stained with Hoechst (blue). Scale bar=20 μm. Similar results were obtained in two independent experiments. (B) Secondary cultured NPCs from the E14 mouse telencephalon were maintained *in vitro* for 72 h without or with 10 μM phenylephrine (PE). After 72 h, cells were fixed and immunostained for tuj1, glial fibrillary acidic protein (GFAP), nestin and galactocerebroside (GC). The number of nestin$^+$, tuj1$^+$, GFAP$^+$ and GC$^+$ cells were counted, and the percentages are presented. Nestin was used as a marker for undifferentiated NPCs. No significant differences were observed.

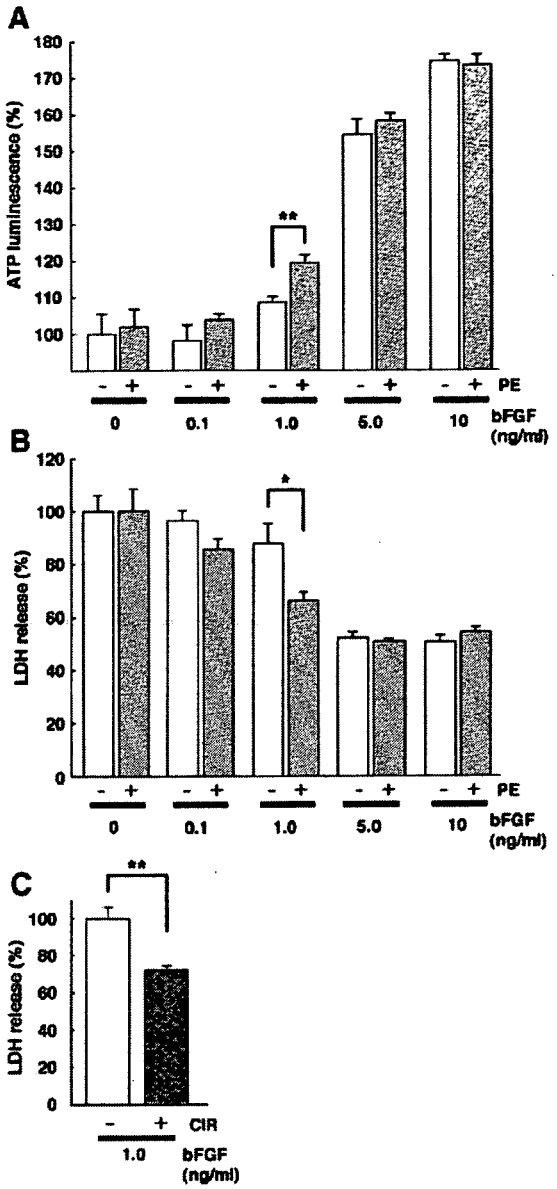

Fig. 3. Effects of α_1-adrenoceptor agonists on the number of cells and cell death of NPCs at various doses of bFGF. Secondary cultured NPCs from the E14 mouse telencephalon were treated without or with 10 μM phenylephrine at different concentrations of bFGF for 24 h. (A) The number of NPCs was examined with an ATP luminescence assay. (B) The viability of NPCs was examined with the LDH release assay. (C) Secondary cultured NPCs from the E14 mouse telencephalon were treated without or with 10 μM cirazoline in 1 ng/ml bFGF for 24 h. Cell survival was assessed by the ATP luminescence assay. Bars represent mean±S.E.M. (n=4). Significant differences are indicated by single or double asterisks (*P<0.05, **P<0.01, Student's t-test).

NPC cultures that contained over 99±0.4% nestin$^+$ undifferentiated NPCs and no more than 0.5% tuj1$^+$ neuronal cells. Using the secondary NPC culture, we examined whether phenylephrine increased the number of NPCs at various doses of bFGF (0~10 ng/ml) using an intracellular ATP luminescence assay (Crouch et al., 1993; Petty et al., 1995). We found that phenylephrine significantly increased the number of NPCs only at a moderate dose (1.0 ng/ml) of bFGF (P<0.01; Fig. 3A) and had no significant effect at high doses (5–10 ng/ml), a low dose (0.1 ng/ml) of bFGF, or no bFGF. To determine whether the effect of phenylephrine on NPCs at 1 ng/ml bFGF was due to promotion of cell growth or cell survival, we examine the effect of phenylephrine on cell death using the LDH release assay (Decker and Lohmann-Matthes, 1988), which measures destruction of the plasma membrane. Phenylephrine also significantly decreased LDH release at 1 ng/ml bFGF (P<0.05; Fig. 3B), indicating that the difference between ATP luminescence (cell numbers) of phenylephrine-treated and

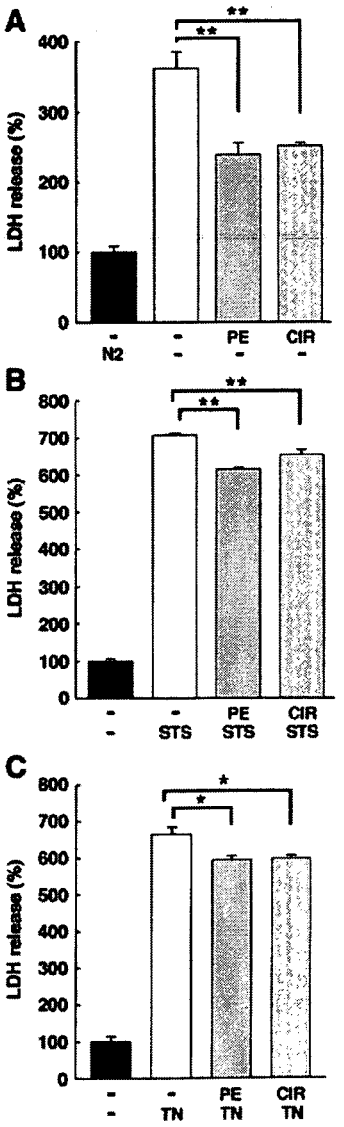

Fig. 4. Phenylephrine and cirazoline promote survival of NPCs under various stress conditions. Secondary cultured NPCs from the E14 mouse telencephalon were incubated in medium lacking N2 (A), 50 nM staurosporine (STS) (B) or 30 ng/ml tunicamycin (TN) (C) in the presence or absence of 10 μM phenylephrine (PE) or 10 μM cirazoline (CIR) for 24 h. Quantification of cell death was performed with the LDH release assay. Bars represent mean±S.E.M. (n=3~5). Significant differences are indicated by single or double asterisks (*P<0.05, **P<0.01, Dunnett's test).

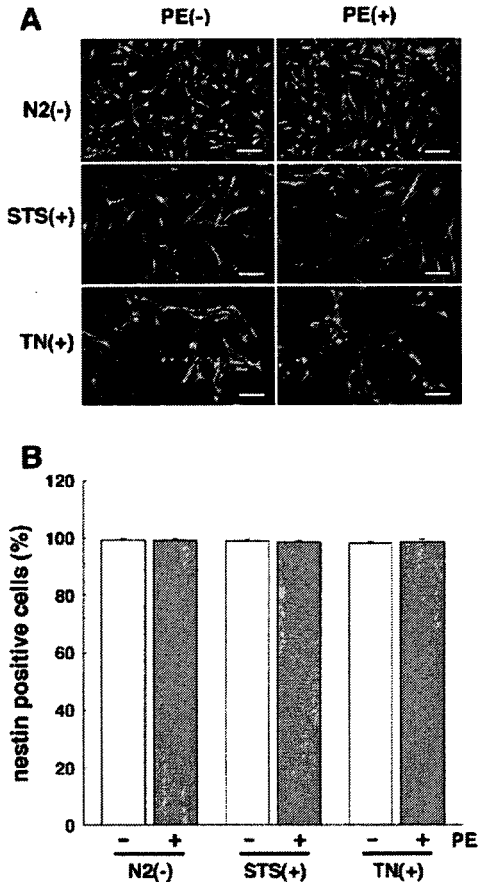

Fig. 5. Effect of phenylephrine on the proportion of nestin-positive cells under various stress conditions. Secondary cultured NPCs were exposed for 24 h to stress conditions without or with 10 μM phenylephrine: N2 deprivation medium, or exposure to 50 nM staurosporine (STS) or 30 ng/ml tunicamycin (TN). After 24 h, the NPCs were fixed and stained with anti-nestin and Hoechst. (A) Fluorescence microscopic images of cells labeled with anti-nestin (green) and Hoechst (blue). Scale bar=50 μm. (B) The percentages of nestin-positive cells in the cultures were quantified. No significant differences were seen among the groups.

untreated NPCs correlated with the difference in the amount of cell death. These results also indicated that phenylephrine protected NPCs from death during bFGF deprivation-induced stress. Moreover, we confirmed that α_1-adrenoceptor agonists specifically protected NPCs from death using another α_1-adrenoceptor agonist, cirazoline. Cirazoline treatment of NPCs under the same culture conditions resulted in a significant decrease in LDH release ($P<0.01$; Fig. 3C), indicating that α_1-adrenoceptor agonists promote survival of NPCs cultured in 1 ng/ml bFGF. A [^{3}H]thymidine incorporation assay showed that phenylephrine and cirazoline did not induce DNA synthesis of NPCs (data not shown).

3.4. α_1-adrenoceptor agonists prevent NPC death upon exposure to various stresses

To determine the extent to which α_1-adrenoceptor agonists could prevent NPC death, we employed other stress conditions: N2 deprivation, or exposure to 50 nM staurosporine or 30 ng/ml tunicamycin. The results of the LDH release assay for these stress conditions showed that N2 deprivation, staurosporine treatment, and tunicamycin treatment induced LDH release from NPCs (361±24%, 706±5% and 664±21%, respectively, relative to the controls; Fig. 4). However, application of the agonists to the NPC cultures under these stress conditions significantly reduced LDH release (N2 deprivation+phenylephrine, 238±18% $P<0.01$; N2

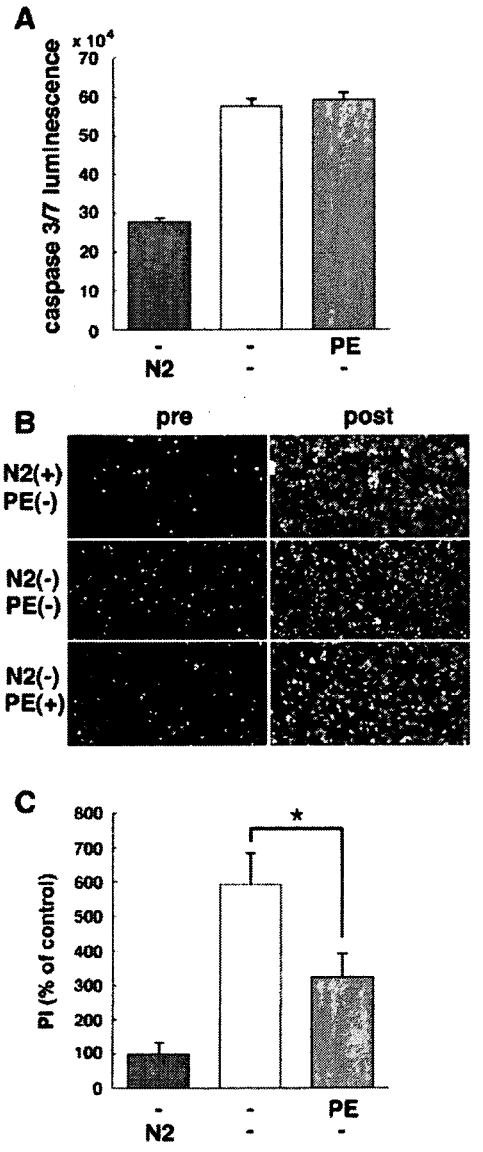

Fig. 6. Phenylephrine does not alter cellular caspase activity but changes propidium iodide penetration into NPCs. Secondary cultured NPCs were incubated without or with 10 μM phenylephrine (PE) under N2 deprivation conditions for 24 h. (A) Caspase-3 and caspase-7 activities in cell lysates were measured by luminometry. (B) Fluorescence microscopy images of dead cells stained with propidium iodide are presented (left). For positive controls, cells were fixed and stained with PI after permeabilization with 0.02% Triton X-100 (right). Scale bar=100 μm. (C) The intensity of propidium iodide staining was measured by fluorometry. Bars represent mean±S.E.M. ($n=4$). Significant differences are indicated by an asterisk (*$P<0.05$, Dunnett's test).

deprivation+cirazoline, 251±5% $P<0.01$; staurosporine+phenylephrine, 614±9% $P<0.01$; staurosporine+cirazoline, 654±16% $P<0.01$; and tunicamycin+phenylephrine, 594±13% $P<0.05$; tunicamycin+cirazoline, 597±10% $P<0.05$) (Fig. 4). Under the three stress conditions, the differences in the efficacies of phenylephrine and cirazoline on LDH release did not differ greatly. However, both agonists were most effective against N2 deprivation stress, where phenylephrine and cirazoline reduced LDH release 34% and 31%, respectively, as compared with the unstressed control (Fig. 4A). These data suggest that α_1-adrenoceptor agonists protected NPC death under several different stress conditions but exhibited different efficacies depending on the particular stress.

3.5. α_1-adrenoceptor agonists do not modulate the proportion of nestin-positive NPCs under stress conditions

Phenylephrine did not affect differentiation of NPCs in cultures with or without bFGF (Fig. 1), and the high proportion (over 98%) of nestin-positive cells remained for ~24 h even in 1 ng/ml bFGF (data not shown). The ability of the agonists to prevent cell death in 1 ng/ml bFGF was thus a direct effect on the nestin-positive NPCs and not an artifact due to contaminating cells. We also examined the effects of stress induced by N2 deprivation, 50 nM staurosporine or 30 ng/ml tunicamycin on NPC differentiation to exclude the possibility that the increased cell numbers observed following α_1-adrenoceptor agonist exposure, as measured by ATP production, were derived from the differentiated cells induced by the stresses. The proportion of nestin-positive NPCs was not changed by N2 deprivation, staurosporine-or tunicamycin-induced stress, and treatment of NPCs with phenylephrine or cirazoline under these stress conditions did not decrease the proportions of nestin-positive cells (Fig. 5).

3.6. Phenylephrine inhibits caspase-3/7-independent cell death

Of the three stress conditions tested, α_1-adrenoceptor agonists most effectively suppressed stress caused by N2 deprivation, as measured by LDH release (Figs. 3 and 4). Whereas cell death induced by bFGF deprivation, staurosporine treatment or tunicamycin treatment probably was caused by activation of various death signaling pathways, the stress caused by N2 deprivation mainly induced caspase-3/7-dependent cell death in NPC cultures (Fig. 6). To ascertain whether α_1-adrenoceptor agonists protect against caspase-3/7-dependent cell death, we examined the effects of α_1-adrenoceptor agonists on cellular caspase-3/7 activities. Stress caused by N2 deprivation induced elevated cellular caspase-3 and caspase-7 activities as compared with non-stress conditions (>2 fold; Fig. 6A). However, the elevated activities of caspases were not changed by treatment of NPCs with phenylephrine (Fig. 6A). Despite a lack of modulation of the cellular caspase activity, phenylephrine suppressed propidium iodide penetration into NPC cytoplasm (45.4%; $P<0.05$, as compared with untreated cells deprived of N2) (Fig. 6B and C). These data indicate that α_1-adrenoceptor agonists selectively protect against caspase-3/7-independent death of NPCs exposed to stress.

4. Discussion

In this study, we prepared highly purified embryonic NPCs (>99% nestin$^+$ cells) from the E14 mouse cortex and found that the cortical embryonic NPCs highly express α_{1A}- and α_{1B}-adrenoceptor genes but express the α_{1D}-adrenoceptor gene at low levels. Our pharmacological experiments also revealed that α_1-adrenoceptor agonists are protective against NPC death induced by various stresses without any modification of the cell differentiation state of the NPCs. Moreover we demonstrated that α_1-adrenoceptor agonists reduced NPC death caused by the N2 deprivation stress without modulation of intracellular caspase-3/7 activities.

The α_1-adrenoceptor is expressed in the ventricular zone and subventricular zone of the embryonic rat forebrain (Pabbathi et al., 1997). The ventricular zone of the embryonic cerebral cortex contains both undifferentiated NPCs and differentiated nascent neuronal cells. Our quantitative RT-PCR analysis showed that purified cortical NPCs express α_{1A}- and α_{1B}-adrenoceptor genes at high levels compared with the E14 embryonic telencephalon, suggesting that the undifferentiated NPCs highly expressed the α_{1A}- and α_{1B}-adrenoceptor genes. We could not confirm the expression of α_1-adrenoceptor proteins in NPCs because of low specificity of commercially available antibodies against α_1-adrenoceptor in immunocytochemical experiments with NPCs (data not shown). However, we demonstrated that α_1-adrenoceptor agonists have protective effects against cell death in NPCs, indicating the presence of the α_1-adrenoceptors in NPCs.

The chemical structure of phenylephrine ((*R*)-3-[1-hydroxy-2-(methylamino) ethyl] phenol) differs from that of cirazoline (2-[(2-cyclopropylphenoxy) methyl]-4, 5-dihydro-1H-imidazole). However, both α_1-adrenoceptor agonists had the same effect on NPC death induced by a moderate concentration (1 ng/ml) of bFGF, nutritional deprivation (no N2 supplementation), staurosporine treatment or endoplasmic reticulum stress (tunicamycin treatment), indicating that the effects were specifically mediated by α_1-adrenoceptors. It is well known that cell death can be induced via multiple apoptosis signaling pathways that are specifically activated by different stresses. Although the α_1-adrenoceptor agonists were able to protect NPCs from death induced by the stresses we tested, the molecular mechanism that underlies this broad protection is unknown. However, treatment of NPCs with α_1-adrenoceptor agonists failed to decrease the activities of caspase-3 and caspase-7, which are activated in the apoptosis pathway. Instead, α_1-adrenoceptor agonists reduced propidium iodide incorporation induced by stress caused by N2 deprivation. These data suggest that α_1-adrenoceptor agonists protect against necrotic NPC death but not apoptotic NPC death.

Phenylephrine or cirazoline protects against cell death induced by bFGF deprivation as well as by STS and nutritional deprivation, or treatment with staurosporine or tunicamycin. Niidome et al. (Niidome et al., 2006) showed that NPC death resulting from growth factor deprivation is caused by both caspase-dependent and -independent pathways in concert with oxidative stress, suggesting that α_1-adrenoreceptor agonists may also protect against NPC death induced by oxidative stresses. On the other hand, application of phenylephrine is effective only against cell death induced by 1.0 ng/ml bFGF. Complete

deprivation of growth factors activates multiple cell death pathways, including apoptosis, necrosis and the oxidative cell death pathway, in cultured NPCs (Niidome et al., 2006). Therefore, the application of phenylephrine is unlikely to be effective against NPC death induced by the overlapping activation of multiple death pathways after complete loss of growth factor support.

In a recent study, Hiramoto et al. (2006) reported that the stimulation of α_1-adrenoreceptors by phenylephrine or by L-epinephrine induces the proliferation of NPCs derived from cultured neurospheres. Our data indicate that α_1-adrenoreceptor agonists do not induce proliferation of purified NPCs. It is known that the neurospheres have the 3D organization in which nestin-positive (progenitor) cells surround a large core of differentiated GFAP-positive (glial) and β-tubulin III-positive (neuronal) cells (Campos, 2004). As such, the NPC cultures prepared from neurospheres could also contain glial and neuronal cells. Thus, the difference between these data may have resulted from differences in the NPC preparation methods and from the purity of the nestin-positive NPCs.

Transplantation of neural stem and progenitor cells into patients with intractable neurological diseases is considered an effective strategy for neural regeneration therapy reviewed in Lindvall et al., (2004). Studies on cell transplantation/implantation for CNS disorders have indicated that neural stem cells and progenitor cells have the ability to replace lost neurons and to repair the damaged nervous system (Chu et al., 2004). However, a large proportion of grafted cells is lost due to early necrotic death. Thus, the low rate of graft survival reduces the effectiveness of such therapies (Emgard et al., 2003). Here we demonstrated that α_1-adrenoceptor agonists protect against NPC death (probably necrotic death) induced by various stresses. We also demonstrated that α_1-adrenoceptor agonists with this protective effect did not modify the cell differentiation state of the NPCs. Thus, α_1-adrenoceptor agonists may be useful for the preparation and maintenance of neural stem and progenitor cells for transplantation therapy, as they are likely to increase cell viability without induction of unexpected cell differentiation. Moreover, phenylephrine is a popular and safe drug that is used as a non-prescription decongestant (Chua and Benrimoj, 1988) Therefore, phenylephrine may be easily applied as an additional reagent in the cultivation medium of neural stem and progenitor cells for transplantation therapy.

Acknowledgments

This work was supported in part by Grants-in-Aid for Scientific Research from the Ministry of Health, Labour and Welfare of Japan, Grants-in-Aid for Scientific Research from the Ministry of Education, Culture, Sports, Science and Technology of Japan, the Program for Promotion of Fundamental Studies in Health Sciences of the National Institute of Biomedical Innovation, and a grant from Japan Science and Technology Agency.

References

Aoki, S., Su, Q., Li, H., Nishikawa, K., Ayukawa, K., Hara, Y., Namikawa, K., Kiryu-Seo, S., Kiyama, H., Wada, K., 2002. Identification of an axotomy-induced glycosylated protein, AIGP1, possibly involved in cell death triggered by endoplasmic reticulum-Golgi stress. J. Neurosci. 22, 10751–10760.

Brewer, G.J., Torricelli, J.R., Evege, E.K., Price, P.J., 1993. Optimized survival of hippocampal neurons in B27-supplemented neurobasal, a new serum-free medium combination. J. Neurosci. Res. 35, 567–576.

Bylund, D.B., Regan, J.W., Faber, J.E., Hieble, J.P., Triggle, C.R., Ruffolo Jr., R.R., 1995. Vascular alpha-adrenoceptors: from the gene to the human. Can. J. Physiol. Pharm. 73, 533–543.

Campos, L.S., 2004. Neurospheres: insights into neural stem cell biology. J. Neurosci. Res. 78, 761–769.

Chu, K., Kim, M., Jung, K.H., Jeon, D., Lee, S.T., Kim, J., Jeong, S.W., Kim, S.U., Lee, S.K., Shin, H.S., Roh, J.K., 2004. Human neural stem cell transplantation reduces spontaneous recurrent seizures following pilocarpine-induced status epilepticus in adult rats. Brain Res. 1023, 213–221.

Chua, S.S., Benrimoj, S.I., 1988. Non-prescription sympathomimetic agents and hypertension. Med. Toxicol. Adverse Drug Exp. 3, 387–417.

Crouch, S.P., Kozlowski, R., Slater, K.J., Fletcher, J., 1993. The use of ATP bioluminescence as a measure of cell proliferation and cytotoxicity. J. Immunol. Methods 160, 81–88.

Decker, T., Lohmann-Matthes, M.L., 1988. A quick and simple method for the quantitation of lactate dehydrogenase release in measurements of cellular cytotoxicity and tumor necrosis factor (TNF) activity. J. Immunol. Methods 115, 61–69.

Emgard, M., Hallin, U., Karlsson, J., Bahr, B.A., Brundin, P., Blomgren, K., 2003. Both apoptosis and necrosis occur early after intracerebral grafting of ventral mesencephalic tissue: a role for protease activation. J. Neurochem. 86, 1223–1232.

Fukazawa, N., Ayukawa, K., Nishikawa, K., Ohashi, H., Ichihara, N., Hikawa, Y., Abe, T., Kudo, Y., Kiyama, H., Wada, K., Aoki, S., 2006. Identification and functional characterization of mouse TPO1 as a myelin membrane protein. Brain Res. 1070, 1–14.

Hieble, J.P., Bondinell, W.E., Ruffolo Jr., R.R., 1995. Alpha- and beta-adrenoceptors: from the gene to the clinic. 1. Molecular biology and adrenoceptor subclassification. J. Med. Chem. 38, 3415–3444.

Hiramoto, T., Ihara, Y., Watanabe, Y., 2006. Alpha-1 Adrenergic receptors stimulation induces the proliferation of neural progenitor cells in vitro. Neurosci. Lett. 408, 25–28.

Lidow, M.S., Rakic, P., 1992. Scheduling of monoaminergic neurotransmitter receptor expression in the primate neocortex during postnatal development. Cereb. Cortex 2, 401–416.

Lidow, M.S., Rakic, P., 1994. Unique profiles of the alpha 1-, alpha 2-, and beta-adrenergic receptors in the developing cortical plate and transient embryonic zones of the rhesus monkey. J. Neurosci. 14, 4064–4078.

Lindvall, O., Kokaia, Z., Martinez-Serrano, A., 2004. Stem cell therapy for human neurodegenerative disorders—how to make it work. Nat. Med. (10 Suppl), S42–S50.

Marien, M.R., Colpaert, F.C., Rosenquist, A.C., 2004. Noradrenergic mechanisms in neurodegenerative diseases: a theory. Brain Res. Brain Res. Rev. 45, 38–78.

Murchison, C.F., Zhang, X.Y., Zhang, W.P., Ouyang, M., Lee, A., Thomas, S.A., 2004. A distinct role for norepinephrine in memory retrieval. Cell 117, 131–143.

Niidome, T., Morimoto, N., Iijima, S., Akaike, A., Kihara, T., Sugimoto, H., 2006. Mechanisms of cell death of neural progenitor cells caused by trophic support deprivation. Eur. J. Pharmacol. 548, 1–8.

Pabbathi, V.K., Brennan, H., Muxworthy, A., Gill, L., Holmes, F.E., Vignes, M., Haynes, L.W., 1997. Catecholaminergic regulation of proliferation and survival in rat forebrain paraventricular germinal cells. Brain Res. 760, 22–33.

Papay, R., Gaivin, R., Jha, A., McCune, D.F., McGrath, J.C., Rodrigo, M.C., Simpson, P.C., Doze, V.A., Perez, D.M., 2006. Localization of the mouse alpha1A-adrenergic receptor (AR) in the brain: alpha1AAR is expressed in neurons, GABAergic interneurons, and NG2 oligodendrocyte progenitors. J. Comp. Neurol. 497, 209–222.

Petty, R.D., Sutherland, L.A., Hunter, E.M., Cree, I.A., 1995. Comparison of MTT and ATP-based assays for the measurement of viable cell number. J. Biolumin. Chemilumin. 10, 29–34.

Popovik, E., Haynes, L.W., 2000. Survival and mitogenesis of neuroepithelial cells are influenced by noradrenergic but not cholinergic innervation in cultured embryonic rat neopallium. Brain Res. 853, 227–235.

Sakurai, M., Ayukawa, K., Setsuie, R., Nishikawa, K., Hara, Y., Ohashi, H., Nishimoto, M., Abe, T., Kudo, Y., Sekiguchi, M., Sato, Y., Aoki, S., Noda, M., Wada, K., 2006. Ubiquitin C-terminal hydrolase L1 regulates the morphology of neural progenitor cells and modulates their differentiation. J. Cell Sci. 119, 162–171.

Slotkin, T.A., Windh, R., Whitmore, W.L., Seidler, F.J., 1988. Adrenergic control of DNA synthesis in developing rat brain regions: effects of intracisternal administration of isoproterenol. Brain Res. Bull. 21, 737–740.

Southwick, S.M., Bremner, J.D., Rasmusson, A., Morgan 3rd, C.A., Arnsten, A., Charney, D.S., 1999. Role of norepinephrine in the pathophysiology and treatment of posttraumatic stress disorder. Biol. Psychiatry 46, 1192–1204.

Zhong, H., Minneman, K.P., 1999. Alpha1-adrenoceptor subtypes. Eur. J. Pharmacol. 375, 261–276.